

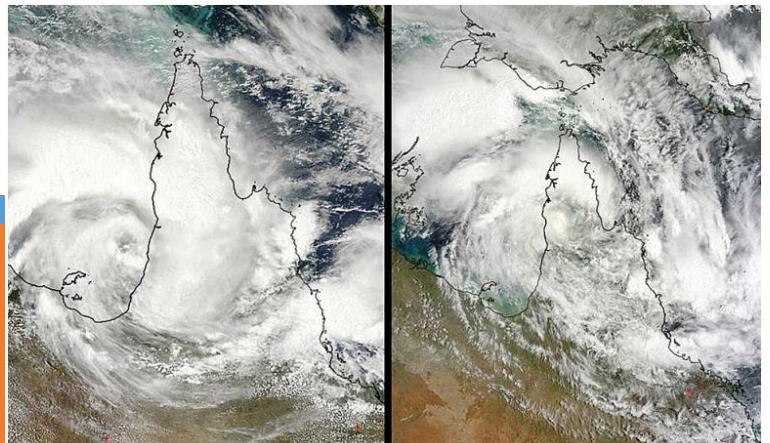
Utilising satellite altimetry data to forecast the coastal impact from tropical cyclones: Cyclone Oswald as a case study

DISSERTATION

PASCALE STILLER
0061046697

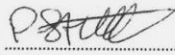
Date: 28th October 2016

Supervisors: Joachim Ribbe and Zahra Gharineiat



Declaration

I certify that the ideas, experimental work, results, analyses and conclusions reported in this dissertation are entirely my own effort, except where otherwise acknowledged. I also certify that the work is original and has not been previously submitted for any other award, except where otherwise acknowledged.

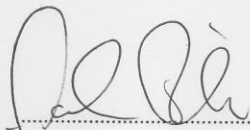

.....

Date: 30/11/16

Signature of Candidate

Pascale Stiller

ENDORSEMENT


.....

Date: 1/12/2016

Signature of Supervisor

Professor Joachim Ribbe

Abstract

Tropical cyclones are one of many climatic phenomena which occur around Australia, forming above the tropical waters around the equator. These systems can have large impacts due to heavy rainfall, storm tides, and strong winds, which can all be produced by tropical cyclones. As storm tides are likely to cause the most damage, the prediction of changes in sea surface height further out to sea during a tropical cyclone would be valuable. The aim of the research completed was to answer the research question "Can satellite altimetry data, combined with coastal tide gauge observations, be utilised to forecast the coastal impact of tropical cyclones?". A focus was placed on tropical Cyclone Oswald, with measured sea surface height, rainfall, and stream discharge along the coast of Queensland during the cyclone presented. A focus was also placed on Hervey Bay, Queensland, with the application of a multivariate regression model to sea level anomaly data measured by tide gauges at Burnett Heads and Rosslyn Bay, along with the sea level variances recorded by satellite altimeters TOPEX/Poseidon, Jason-1 and Jason-2 off the coast of Queensland. The results of the model showed a correlation of approximately 0.6 around the tide gauges used, and the two tests of the performance of the model determined that the model performed well in these areas. When compared to what occurred during Oswald around Hervey Bay, the measured data was able to be explained by the model. As a result, the model was proven to be able to be applied. Further research into how the number of tide gauges and the data used can improve the results of the model could be completed into the future.

Cover image: Satellite images of tropical cyclone Oswald as it made landfall north of Kowanyama, Queensland (BOM 2014)

List of Figures

Figure 1.1 – Locations of the major climatic drivers across Australia.....	1
Figure 1.2 – Map of Hervey Bay.....	4
Figure 2.1 – The tracks of tropical cyclones around Australia from 1989/90 to 2002/03.....	13
Figure 2.2 – The number of tropical cyclones to at least graze the coast along Brisbane, as well as the values of the Southern Oscillation Index (SOI), which is linked to ENSO. The red line is the five year running average.....	19
Figure 2.3 – Path of tropical Cyclone Oswald across the eastern side of Australia.....	21
Figure 2.4 – Amount of rainfall for the week ending 29th January 2013.....	22
Figure 2.5 – The distribution of rainfall for January 2013. The blue sections indicate areas where the amount of rainfall was higher than average, and the red sections indicate the areas where rainfall was lower than average.....	23
Figure 3.1 – Locations of tide gauges. The red points represent the three tide gauges used for the model and validation.....	25
Figure 3.2 – Locations of the data collected by the satellite altimeter tracks around Queensland, shown as the blue lines.....	26
Figure 3.3 – Locations of selected rainfall measuring stations.....	28
Figure 3.4 – Locations of stream discharge measurement stations. The names consist of the river the station is on and the name of the station in brackets.....	29

Figure 4.1 – Daily mean SSH in metres, measured by tide gauges during tropical Cyclone Oswald. Any days which did not have a full day of data were not included. Graphs are ordered in terms of their positioning along the coastline, starting from Darwin and moving to the right. The y-axis is not in the same range across the graphs, however, the increments of the axis have been kept the same for comparison.....33 – 35

Figure 4.2 – Daily total rainfall in millimetres, measured during tropical Cyclone Oswald. Any measurements which contain more than one day’s worth of data have not been included. The graphs are ordered in terms of their positioning along the coastline, starting from Stokes Hill and moving to the right. The y-axis across the graphs are not the same range, but they all are in increments of 50 mm to help with the comparison.....36 – 37

Figure 4.3 – Daily total stream discharge in megalitres per day, measured during tropical Cyclone Oswald. They are ordered in terms of their positioning along the coastline, starting from Norman River (Glenore Weir) and moving to the right. The y-axis across the graphs are not the same range.....39 – 40

Figure 4.4 – Distribution of temporal correlation coefficients (Burnett Heads only) – (a) predicted and (b) measured.....41

Figure 4.5 – Distribution of temporal correlation coefficients (Burnett Heads and Rosslyn Bay) – (a) predicted and (b) measured42

Figure 4.6 – RMS^{ϵ} - (a) Burnett Heads only and (b) Burnett Heads and Rosslyn Bay.....43

Figure 4.7 – Hindcast skill – (a) Burnett Heads only and (b) Burnett Heads and Rosslyn Bay45

Figure 4.8 – Comparison of measured SLAs at Urangan and predicted SLAs using (a) Burnett Heads only and (b) Burnett Heads and Rosslyn Bay.....47

List of Tables

Table 1.1 – Definitions of the major climatic drivers across Australia.....	2
Table 2.1 – The major extreme weather events which occur in and around Australia, as well as the duration time of these events.....	5
Table 2.2 – Major categories of tropical cyclones and other low pressure systems with high wind speeds.....	12
Table 2.3 – Australian tropical cyclone category system.....	14
Table 3.1 – Information about selected tide gauges.....	25
Table 3.2 – Information about selected rainfall measuring stations.....	28
Table 3.3 – Information about selected stream discharge measuring stations.....	29

Table of Contents

1	Introduction	1
2	Literature Review	5
2.1	Introduction	5
2.2	Extreme Weather of Australia	5
2.2.1	Heatwaves	6
2.2.2	Drought	7
2.2.3	Bushfires	7
2.2.4	Heavy Rainfall	8
2.3	Tropical Cyclones	8
2.3.1	Formation to Dissipation	8
2.3.2	Extratropical Cyclones	10
2.3.3	East Coast Lows	10
2.3.4	Tropical Cyclone Classification	11
2.3.5	Tropical Cyclones Around Australia	12
2.3.6	Monitoring of Tropical Cyclones Around Australia	14
2.3.7	Effect of Tropical Cyclones on Coastal Communities	16
2.3.8	South-East Queensland Tropical Cyclones	18
2.4	Tropical Cyclone Oswald	20
3	Data and Methodology	24
3.1	Data	24
3.1.1	SSH - Tide Gauge	24
3.1.2	SSH - Satellite Altimeters	26
3.1.3	Rainfall Data	27
3.1.4	Stream Discharge Data	28
3.2	Method	30
4	Results	33
4.1	Tropical Cyclone Oswald	33
4.1.1	Tide Gauge Data	33
4.1.2	Rainfall Data	36
4.1.3	Stream Discharge Data	39
4.2	Multivariate Regression Model	41
4.2.1	Distribution of Temporal Correlation Coefficients	41
4.2.2	Tests of Performance	43

4.2.3	Validation	46
5	Discussion	50
5.1	Multivariate Regression Model	50
5.2	Limitations	50
5.3	Improvements/Future Directions.....	51
6	Conclusion.....	53
7	Bibliography.....	54

1 Introduction

Australia is a continent which experiences a number of different climate patterns across the country as well as a variability in this climate (Figure 1.1, Table 1.1). Across the northern region of the country, weather and climate are affected by tropical weather systems and phenomena of climate variability. This includes the Madden-Julien Oscillation (MJO), the El Niño Southern Oscillation (ENSO), and the Indian Ocean Dipole (IOD). The southern parts of Australia are impacted by extratropical systems, including blocking highs and cut-off lows, and climate variability is driven by the Southern Annular Mode (SAM), and changes in the location of the subtropical ridge (CSIRO & BOM 2015).

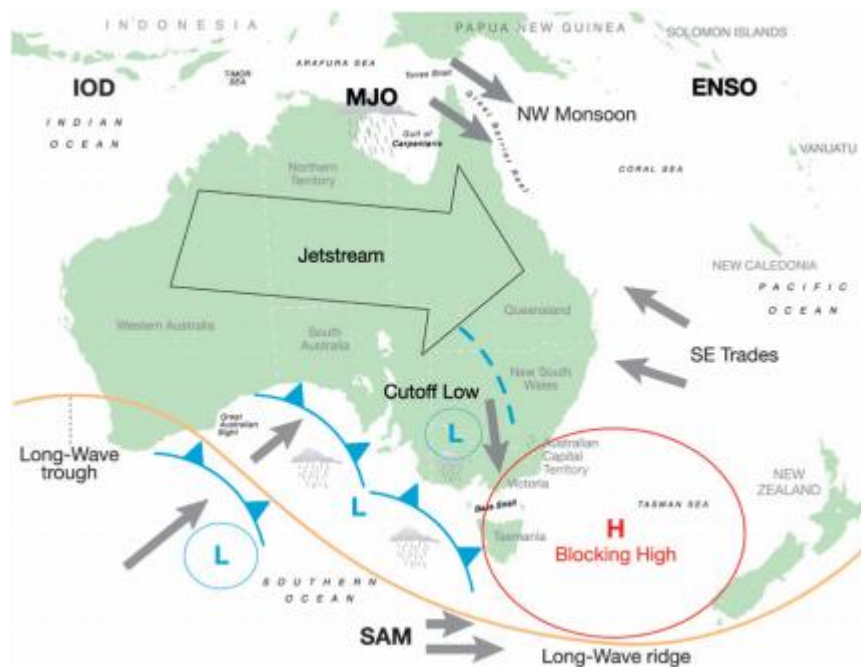


Figure 1.1 – Locations of the major climatic drivers across Australia (Source: Risbey et al. 2009)

Table 1.1 – Definitions of the major climatic drivers across Australia (Source: CSIRO & BOM 2015)

Name	Definition
Madden-Julien Oscillation	A highly convective disturbance which travels eastward to the north of Australia
El Niño Southern Oscillation	An interaction between the temperature of the Pacific Ocean and the atmosphere to the north-east of Australia
Indian Ocean Dipole	A dipole across the Indian Ocean, where the phase is determined by the polar changes in sea surface temperature between the eastern and western Indian Ocean
Blocking Highs/Cut-Off Lows	Bands of high/low pressure systems which alter the atmospheric circulation around the south-east of Australia
Southern Annular Mode	A westerly atmospheric circulation to the south of Australia caused by variation in the mass of the atmosphere
Subtropical Ridge	A band of high pressure to the south of Australia which circles the globe

Of the drivers mentioned above, the one which has one of the largest influences on Australian weather and climate, particularly rainfall across eastern Australia, is ENSO (Risbey

et al. 2009). ENSO is driven by the temperature of the equatorial Pacific Ocean and its interaction with the atmospheric circulation (Chiew et al. 1998). The three states which ENSO can be in are El Niño (warmer sea surface temperature (SST) in the Pacific, less than average rainfall across eastern Australia), La Niña (cooler SST in the Pacific, more than average rainfall across eastern Australia) and neutral (Meyers et al. 2007). These states can be determined using a number of indices relating to the atmosphere and the SST. The index which is the most widely used is the Southern Oscillation Index (SOI), which is the difference in air pressure at the surface between Tahiti and Darwin (Risbey et al. 2009).

All of these climatic drivers are capable of influencing extreme weather events across Australia (CSIRO & BOM 2015). One such extreme event is a tropical cyclone (Emanuel 2003). These events can be catastrophic, resulting in millions of dollars in damage to infrastructure as well as loss of life (Middelmann 2007). Tropical cyclones can also push natural processes and systems to their limit, causing flooding and landslides (Chan 2005). The main factors of tropical cyclones which cause damage are severe winds, heavy rainfall and storm tides, with storm tides being capable of causing the most damage (Middelmann 2007).

One way storm tides can be monitored is through the use of tide gauges. Tide gauges are located along the coastline and calculate the average sea surface height (SSH), known as the Mean Sea Level (MSL), across set intervals (PCTMSL 2011). Further out to sea, the SSH is measured through the use of satellite altimeters, taking measurements approximately every ten days (Lambin et al. 2010). As tropical cyclones can last from a number of days to a couple of weeks (Middelmann 2007) it means that the tropical cyclones may pass through the area before the satellite altimeter is in position to collect data. As a result, it would be

beneficial for altimetry data to be available in hourly intervals, through the combination of satellite altimetry data and tide gauge data. This would lead to predicting changes in SSH due to tropical cyclones further from the coastline in smaller increments of time, resulting in better warning times of imminent storm tides.

The following dissertation addresses the research question “Can satellite altimetry data, combined with coastal tide gauge observations, be utilised to forecast the coastal impact of tropical cyclones?”. This will be achieved through the use of a multivariate regression model (Høyer & Andersen 2003). It will follow a similar method to that presented by Deng et al. (2015), although a smaller number of tide gauges will be used. A focus will be placed on tropical cyclone Oswald, which travelled along the Queensland and New South Wales coast from the 17th to the 29th January 2013 (BOM 2014). In particular, the changes in SSH around Hervey Bay (Figure 1.2) which occurred during this cyclone will be investigated.

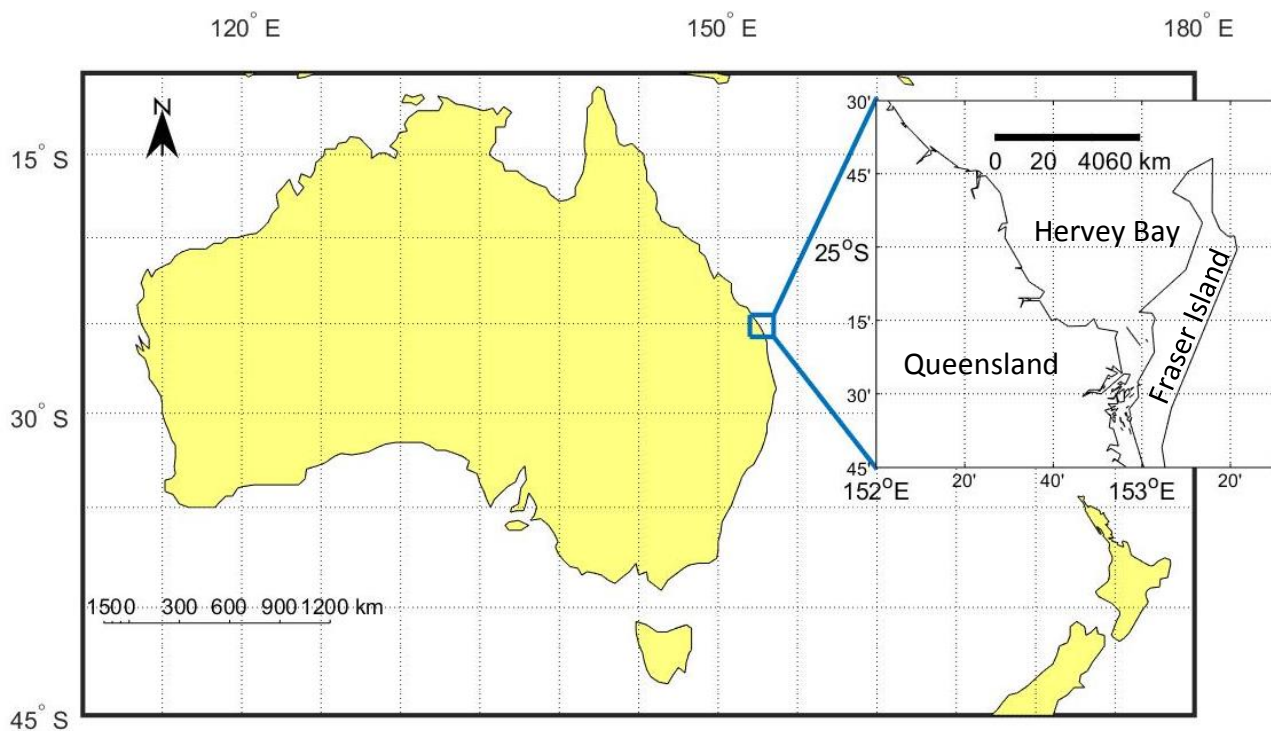


Figure 1.2 – Location and map of Hervey Bay

2 Literature Review

2.1 Introduction

In the following literature review, a focus will be placed on tropical cyclones. This includes what cyclones are, the formation process, classification systems, as well as the tropical cyclone season of Australia and the effect the presence of a cyclone has on coastal communities. Both Hervey Bay and the effects of tropical cyclones to this area, as well as tropical cyclone Oswald, will also be mentioned. This will be preceded by an overview of the extreme weather events in Australia which influence rainfall across the continent (Table 2.1). This is to demonstrate where tropical cyclones fit compared to other events, in terms of duration of event, amount of rainfall and damages caused.

Table 2.1 – The major extreme weather events which occur in and around Australia, as well as the duration time of these events (Sources: Leigh et al. 2015; Pepler, Coutts-Smith & Timbal 2014)

Name of Event	Time Scale
Heatwaves	Days - Weeks
Drought	Months - Years
Bushfires	Hours - Days
Heavy Rainfall	Hours - Days
Tropical Cyclones	Days - Weeks

2.2 Extreme Weather of Australia

In Australia, an extreme weather event is an event which is considered to be rare for the period of time it occurs in (Arblaster et al. 2015). One aspect of weather which falls into this category is rainfall, where extreme events can span from hours to years. Events which are caused by less than average rainfall include heatwaves and droughts, with both events

capable of producing the right conditions for a third extreme event – bushfires. Heatwaves and droughts can occur simultaneously (since heatwaves occur on a smaller time scale to droughts), one can be a result of the other, or the two events can be unrelated (Leigh et al. 2015).

There are also two extreme weather events in Australia which are a result of more than average amounts of rainfall. These are heavy rainfall events and tropical cyclones. All of these events can cause flooding, which is another extreme event which occurs in Australia (Leigh et al. 2015). Tropical cyclones will be covered in section 2.3.

2.2.1 Heatwaves

A heatwave is defined as a period of at least three consecutive days in which both the maximum and minimum temperatures exceed the expected conditions for that period (Leigh et al. 2015). Heatwaves are caused by the presence of blocking highs, a band of high pressure systems which form around the southern part of Australia. When situated around the south-eastern side of Australia, these highs cause northerly winds to form, whereas a band situated around the southern part causes easterly winds to form. These winds result in low rainfall and an increase in temperature. Heatwaves can be linked to the condition of ENSO, IOD and SAM (Purich et al. 2014).

An example of a heatwave which severely affected Australia is one which occurred across Victoria during January and February in 2009. This event is currently one of the longest heatwave events to occur in the area, and broke a number of maximum temperature records (Perkins-Kirkpatrick et al. 2016). After almost two weeks of high temperatures (reaching above 45°C), little to no rainfall and strong winds, the hot and dry conditions across Victoria on the 7th of February resulted in the most devastating bushfires in

Australian recorded history. This event is known as the 'Black Saturday' bushfires, where more than 150 people were killed and entire towns were severely damaged (Engel et al. 2013).

2.2.2 Drought

A drought is a period of time in which the amount of rainfall recorded is less than what is expected for that period (Leigh et al. 2015). Since there is less moisture available, it can also mean an increase in temperatures, which increases the rate of evaporation. This can be devastating, particularly when it occurs across areas which focus on agriculture. This is due to the fact that agriculture has a large reliance on water supply. Drought conditions have been linked to the state of ENSO and IOD (Ummenhofer et al. 2011).

One drought which has affected Australia in the past is the Millennium Drought, which mainly occurred across the southeast of Australia between 2001 and 2009. It is believed to be one of the driest periods that has impacted the area, causing major problems for agriculture as this sector relies heavily on water. There were also a number of bushfires which occurred as a result of the drier conditions (van Dijk et al. 2013).

2.2.3 Bushfires

Bushfires are fires which occur in areas of vegetation and have not occurred due to human intervention (deliberately lit) (Steffen, Hughes & Karoly 2013). The ideal conditions for a bushfire to occur is hot and dry weather, combined with a strong wind (Leigh et al. 2015). If the ideal conditions are met, the fires can spread quickly across large distances. As a result, natural environments, man-made structures and human beings can be caught in the fires and destroyed or lost. This includes damage from the heat and the smoke given off by the fire (Haynes et al. 2010; McAneney, Chen & Pitman 2009).

2.2.4 Heavy Rainfall

Heavy rainfall is a prolonged or intense period of rainfall which is above the average amount of rainfall in the area. These rainfall events can lead to flooding due to catchment areas being unable to cope with the excess amounts of water. Heavy rainfall can also be beneficial, particularly when it occurs after a drought period. This is due to these events providing large amounts of water, which can help with water availability (Steffen, Hughes & Karoly 2013).

2.3 Tropical Cyclones

2.3.1 Formation to Dissipation

Over the warm, tropical oceans surrounding the equator, tropical cyclones form from low pressure systems (Steffen, Hughes & Karoly 2013), with the system itself capable of spanning anywhere between 500 and 1000km across (Chan 2005). Formation occurs during the summer and autumn seasons in the respective hemisphere, driven by heat transfer from the water (Emanuel 2003). The SST needs to be greater than approximately 26°C, with the length of the pre-formation period dictating what the exact minimum temperature can be (Dare & McBride 2011).

The formation of a tropical cyclone starts when there is a disturbance in the atmosphere, and the absolute vorticity of the flow of air is not equal to zero (Emanuel 2003). The absolute vorticity is the sum of the earth's vorticity (caused by the rotation of the planet) and the relative vorticity (caused by moving air) (Saha 2010). The ocean water, evaporating due to the high sea surface temperature, travels upwards into the atmosphere, where the energy, stored as latent heat, is then released. This creates a convective current, as the now cooler air travels back towards the ocean. The centre of the tropical cyclone forms into a

vortex, with the air in the lower sections flowing around the vortex in a clockwise direction in the southern hemisphere and an anticlockwise direction in the north. Towards the top of the vortex, however, the flow of air is in the opposite direction (Chan 2005).

This means that tropical cyclones form in a distinct shape. The centre of the cyclone is referred to as the eye, where both the wind speeds and the atmospheric pressure at the surface are minimal. The eye is not in the same state as the rest of the tropical cyclone, and is usually calm in comparison. This eye is surrounded by the vortex, which is also known as the eye wall. This is where the heaviest rainfall and wind speeds tend to occur (Granger et al. 2001).

The rotation of the system causes the clouds around the eye wall to form what is known as rainbands. These are bands of cloud which, due to the strength of the vertical circulation and the strong winds around the eye wall, are pulled towards the centre of the tropical cyclone. Typically, rainbands span more than 1000 kilometres across (Granger et al. 2001).

For the majority of cyclones, formation occurs from at least five degrees North and South from the equator. Tropical cyclones forming any closer to the equator are rare, although if the conditions are favourable it is possible for formation to occur. These cyclones tend to be very weak and do not last very long (Emanuel 2003).

Once formed, tropical cyclones travel away from the equator. Cyclones will gain momentum during travel, but only as long as the temperature at the surface remains above approximately 26°C and the cyclone does not interact with other atmospheric circulations. If these conditions are no longer met, the tropical cyclone will instead start to dissipate (Emanuel 2003). One of the main examples of the conditions not being met is when the

surface is no longer warm enough, which is due to a lower sea surface temperature or the tropical cyclone moving onto land (Steffen, Hughes & Karoly 2013).

2.3.2 Extratropical Cyclones

If a tropical cyclone reaches the mid-latitudes and decay has started, it is possible for the cyclone to interact with upper level troughs. The temperature within these troughs are much colder compared to the tropical cyclone and, as a result, it is possible for the two systems to interact with each other. When interacting with a tropical cyclone, these troughs can either have no effect due to the cyclone not passing close enough; cause the cyclone to decay further due to the colder temperature; or cause the cyclone to go through an extratropical transition and become an extratropical cyclone (Granger et al. 2001).

An extratropical cyclone is a tropical cyclone which has changed in nature and no longer follows all the characteristics of a tropical cyclone. The cool air of the upper-level trough interacts with the warm air within the tropical cyclone and, as a result, the energy release from the heat increases. This is an extratropical transition. The cyclone itself loses its shape slightly, becoming more asymmetrical, and the intense conditions around the eye of the cyclone spreads outwards into the rain bands. This creates a more intense storm and can result in large amounts of rainfall, higher wind speeds, an increase in storm surges, and an increase on overall speed, before the tropical cyclone decays completely (Jones et al. 2003).

2.3.3 East Coast Lows

An east coast low is a low pressure system which forms over waters to the east of a body of land in the mid-latitudes (Pepler, Coutts-Smith & Timbal 2014). The formation of these low pressure systems in Australia is to the east of Queensland and New South Wales, with the Great Dividing Range forming the western boundary of the area. Formation occurs several

times a year on average, with a higher probability of the systems occurring during the cooler months. Other than this, these low pressure systems show similar characteristics to tropical cyclones (Ji et al. 2015).

2.3.4 Tropical Cyclone Classification

Tropical cyclones can have different names, depending on the region in which formation occurs. In the western North Atlantic and eastern North Pacific tropical cyclones are known as hurricanes, while in the western North Pacific the term typhoon is used. A severe tropical cyclone is what tropical cyclones are referred to as in all other applicable areas (Chan 2005).

When it comes to categorising tropical cyclones, the main basis for categorisation is the maximum wind speed (Table 2.2). As a tropical cyclone is forming, the United States measure the wind speed over ten metres for one minute, while all other areas measure horizontal wind speed over ten metres for ten minutes. Typically, tropical cyclones which fall into the >32 m/s category are the only cyclones which show the presence of an eye along with the cloud pattern, although some tropical storms can show some indication of this formation (Emanuel 2003).

Table 2.2 – Major categories of tropical cyclones and other low pressure systems with high wind speeds
(Source: Emanuel 2003)

Name	Wind Speed (m/s)
Tropical Depression Tropical Low	<= 17
Tropical Storm	18 to 32
Severe Tropical Cyclone Hurricane Typhoon	> 32

Once a tropical cyclone has reached a land mass, its movement can be described in one of two ways. A tropical cyclone is considered to have made landfall when the eye of the storm has crossed over from the water onto land. Any tropical cyclone where the eye is within 500 kilometres of the shoreline and does not make landfall is considered to be “grazing the shoreline” (Dare 2013).

2.3.5 Tropical Cyclones Around Australia

Australian tropical cyclones form in the southern Pacific and southern Indian Oceans to the north of the continent (Emanuel 2003) (Figure 2.1). The official tropical cyclone season in Australia is from November to April of the following year (CSIRO & BOM 2015), although it is possible for tropical cyclones to form outside this time range. During the season, it is possible for tropical cyclones to contribute up to half of annual rainfall in certain areas, particularly around the northern and north-western areas of Australia (Dare 2013). This is the same time period during which the northern areas of Australia experience the wet

(monsoon) season, which is a cycle of more than average rainfall followed by no rainfall, which then repeats itself until the end of the season (CSIRO & BOM 2015).

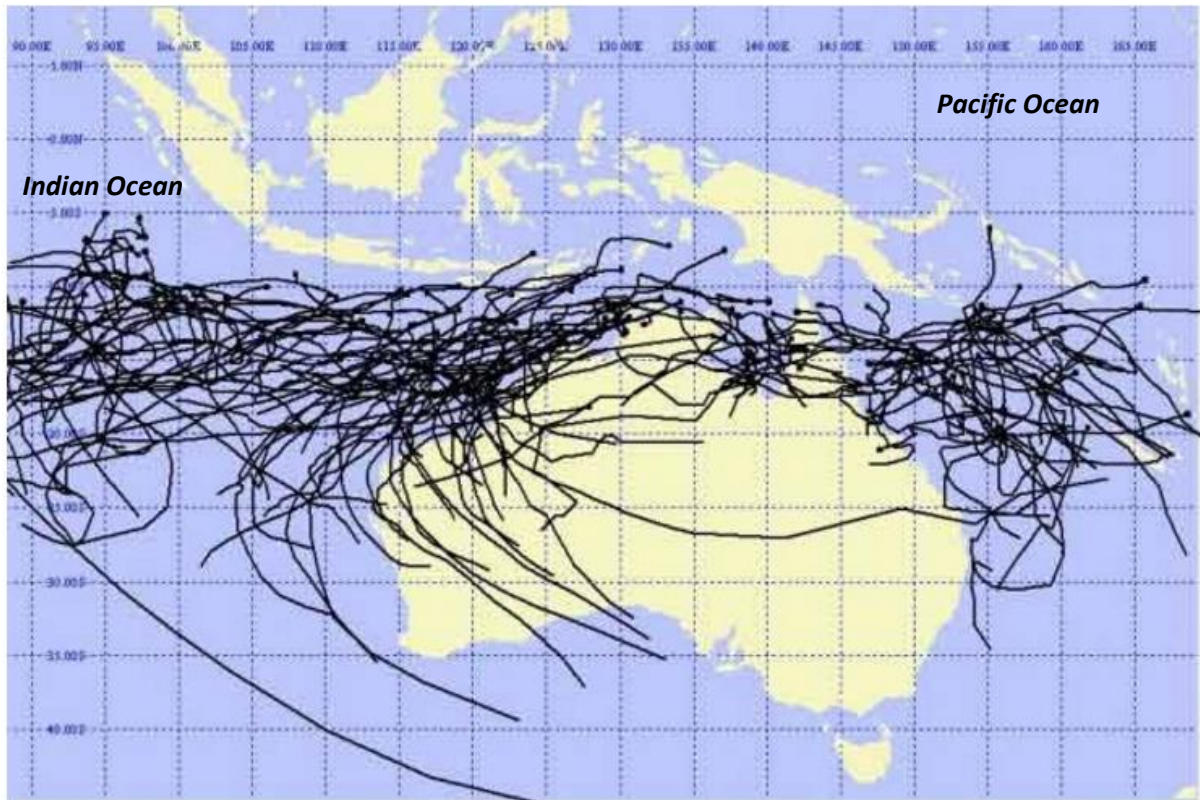


Figure 2.1 – The tracks of tropical cyclones around Australia from 1989/90 to 2002/03 (Source: BOM 2003)

For tropical cyclones around Australia, the classification system which is used describes tropical cyclones which have maximum wind speeds above 32 m/s. In total, this system has five categories (Table 2.3). Any tropical cyclone which is classified as a Category 3 or above is referred to as a severe tropical cyclone. Category 1 and 2 cyclones are referred to as a tropical cyclone. Depending on what the maximum wind speed is, the classification can interchange between categories as it gains or loses energy due to changing conditions, or drop out of this classification system completely and form a tropical storm or low (Granger et al. 2001).

Table 2.3 – Australian tropical cyclone category system (Source: Granger et al. 2001)

Category	Wind Speed (km/h)	Wind Speed (m/s)
Category 1	115 to 125	32 to 35
Category 2	125 to 170	35 to 47
Category 3	170 to 225	47 to 63
Category 4	225 to 280	63 to 78
Category 5	>280	>78

Due to the influence of ENSO on Australia’s climate, the state of ENSO has some effect on the amount of rainfall during the tropical cyclone season. Dare (2013) found that, of the seven tropical cyclone seasons which produced the largest volume of seasonal rainfall in the period 1969 to 2010, four were during a neutral ENSO phase, while the rest were during a La Niña phase. For the seven seasons with the lowest volume of seasonal rainfall across the same period, the situation was the opposite, with an El Niño phase being associated with more than half. Due to high interannual variability for each ENSO phase however, this connection is only likely (Dare 2013). Villarini and Denniston (2016) found a similar result, concluding that an area has a high probability of reaching a larger than normal annual rainfall due to tropical cyclones during a La Niña phase.

2.3.6 Monitoring of Tropical Cyclones Around Australia

In Australia, there are a number of ways in which tropical cyclones are detected and tracked from the early stages of formation to the end of their decay. Since the 1960s, the use of satellite imagery has been one of the main forms of both detecting and tracking cyclones (Granger et al. 2001). This is through the use of the Dvorak technique, which is a system used internationally (Knaff et al. 2010).

The Dvorak technique starts by using satellite imagery to locate the eye of the cyclone. If an eye is found, the features of the tropical cyclone are mapped. From here, infrared sensors on the satellites capture the temperature of the highest cloud layer within this mapped formation. An estimate of intensity is then calculated through the use of a scale from one to eight, with one being the lowest intensity. This is then matched to a corresponding maximum wind speed (Knaff et al. 2010).

The tracks of cyclones can be determined through the use of forecasting tools. These forecasting tools combine data and patterns from tropical cyclones which have formed and passed through the same general area. This includes the time of the year the tropical cyclone formed, the properties it displayed and the general path it took. These factors need to match the current tropical cyclone to a high degree of accuracy, as this will result in a more accurate prediction. Also, different forecasting tools can result in predictions for a number of different time scales, varying from a few hours to a number of days (Roy & Kovordányi 2012).

The effects of tropical cyclones can also be monitored. This involves collecting data to form an overview of the tropical cyclone and its damage, as well as initiate warning systems for extreme and dangerous conditions. One such measurement is the sea surface height.

Around the coast, tide gauges are positioned to capture the height of the waves (SDMG 2013). Tide gauges measure the sea level height through comparison of their position to a nearby fixed point on the land. The use of Global Positioning System (GPS) is also applied, as it is possible for the fixed points to move slightly in the vertical plane through natural processes (Collilieux & Wöppelmann 2010).

The SSH can also be measured from further out to sea through the use of satellite radar altimeters (Shum, Ries & Tapley 1995). These satellites are placed in a set orbital path 1336km above the earth's surface on an inclination of 66°, with a set distance between tracks (approximately 300 km at the equator). When newer satellites are launched, they are placed on the same orbit path as their predecessors with approximately one minute of time between them, to calibrate the accuracy of both altimeters. Once calibrated, the older satellite is moved to a different point in the orbit, where it continues to collect data alongside the new satellite until it is decommissioned (Lambin et al. 2010).

The altimeters, which are sensors attached to the satellite, send a radar pulse to the surface of the water and back to the satellite. The amount of time this takes is measured, and the distance between the satellite and the surface can then be calculated. The changes in the distance can be explained by a slight change of orbit by the satellite or a change in SSH (Shum, Ries & Tapley 1995). This method can also be used to calculate wind speed through the number of radar pulses which return to the satellite as well as the changing wave height due to the wind (Zhao & Toba 2002).

One downside of using satellite altimetry data is that the data measured close to the coastlines of land masses tends to be of a lower quality. This can be caused by the high deviations of SSH around the coastline and/or the shallower waters, which interfere with the reflection of the radar pulse. These errors are called shallow-water gravity anomalies (Hwang & Hsu 2008).

2.3.7 Effect of Tropical Cyclones on Coastal Communities

Once a tropical cyclone starts to travel towards or around land masses, coastal communities can be greatly impacted. The presence of the tropical cyclone can drastically change

conditions both along the coastline as well as further inland, due to excessive rainfall, changes in pressure and strong winds. Low-lying communities can be the most affected in these situations (Steffen, Hughes & Karoly 2013).

One of the impacts which can occur, to low-lying communities in particular, is changes in the SSH along the coast (Steffen, Hughes & Karoly 2013). When a tropical cyclone is present, a combination of the strong winds and the low pressure from the system causes the water to be displaced towards the coast. This is referred to as a storm surge (Granger et al. 2001). Due to this increase in SSH, the water is capable of travelling further inland. As a result, flooding can occur (Steffen, Hughes & Karoly 2013).

The tide level can then increase the SSH further (Steffen, Hughes & Karoly 2013). Tides, which occur due to the gravitational pull between the earth and the moon, follow a distinct pattern vertically between a high tide (tide height at its highest point) and low tide (tide height at its lowest point). This cycle between the two levels occurs approximately twice a day (Hicks 2006). The combination of the tide level and a storm surge is called a storm tide. Storm tides can also cause flooding, with more water travelling inland the closer the tide level is to high tide (Steffen, Hughes & Karoly 2013).

Along with storm surges and storm tides, rainfall associated with tropical cyclones can cause flooding to occur. Flooding due to tropical cyclones is the most common factor involved with these storms. In water catchment areas within the vicinity of the coastline, the excessive amount of rainfall can cause river systems, dams, and other water catchment areas to exceed their capacity. As the water cannot be contained at this point, the surrounding areas can experience flooding. This can be amplified through the flooding

which is also caused by storm surges and storm tides, leading to flooding occurring from two different directions at once (Steffen, Hughes & Karoly 2013).

Another part of tropical cyclones which affects coastal communities is the winds. These winds can reach very high speeds, with the most intense cyclones in Australia capable of 280 km/h and above. Australian tropical cyclones with winds above 130 km/h, associated with (the centres of) Category 3 cyclones and higher, are more likely to cause large amounts of damage. This is due to the strong wind being able to break apart infrastructure, uproot trees, and throw heavier debris across large distances with a great amount of force behind it. These winds cause large amounts of damage to property through both the wind itself and the items picked up and thrown by the wind. Also, the strong winds can persist for longer periods if the cyclone is in the same area for an extended period of time, which can continue to cause damage (Granger et al. 2001).

One example of a tropical cyclone which caused large amounts of damage to the coastal communities is tropical Cyclone Tracy. Tracy made landfall at Darwin in December of 1974 (Middelmann 2007), breaking the record for the highest storm surge in the area (Granger et al. 2001). As a result, Tracy is currently the most costly tropical cyclones in Australian history (Middelmann 2007), with just under 90% of the total costs being from damages to buildings (Haigh et al. 2013).

2.3.8 South-East Queensland Tropical Cyclones

One area of Australia which is affected by tropical cyclones is south-east Queensland. In reference to the capital of Queensland, Brisbane, the average number of tropical cyclones to pass at least at grazing distance to the city is equal to approximately one per season (Figure

2.2). The total cyclones which at least graze the coast of Brisbane per year can be anywhere between zero up to seven (Granger et al. 2001).

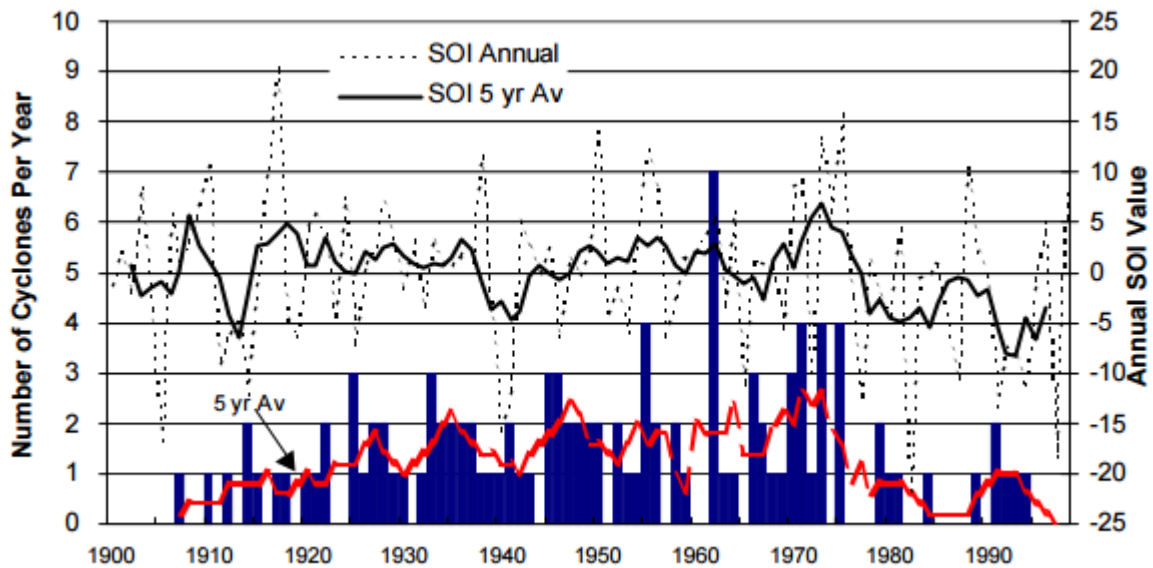


Figure 2.2 – The number of tropical cyclones to at least graze the coast along Brisbane, as well as the values of the Southern Oscillation Index (SOI), which is linked to ENSO. The red line is the five year running average (Source: Granger et al. 2001)

As south-east Queensland is below the lower edge of the formation zone, the tropical cyclones can be at varying strengths once they reach the area. If the cyclone formed near the top of the formation zone, it is possible for the system to have travelled a large distance over water, gaining in strength. It is also possible for the cyclone to be losing strength, due to changing conditions. This decrease in strength can then cause the low pressure system to be classified as a tropical low (Granger et al. 2001).

One area of south-east Queensland which has had an effect from tropical cyclones is Hervey Bay. During February in 1992, tropical Cyclone Fran passed through the area, causing massive flooding along the Mary River. This was the second flood in a matter of weeks, as an earlier flood had resulted from extensive amounts of rainfall. Due to these two floods, approximately 1000 km² of seagrass, which grows in shallow waters around the bay, was

damaged and/or destroyed (Preen, Lee Long & Coles 1995). The dugong population in the area suffered as a result, as the dugongs were unable to access enough food (Preen & Marsh 1995).

Once reaching the south-east Queensland area, tropical cyclones may start to interact with upper-level troughs which travel in a westerly direction. As a result, this is the main area across the eastern side of Australia for tropical cyclones to transition into extratropical cyclones and build in strength. An example of a cyclone which underwent an extratropical transition in this area is tropical Cyclone Lance in April of 2004, which occurred to the east of Brisbane (Granger et al. 2001).

2.4 Tropical Cyclone Oswald

Tropical Cyclone Oswald was one of many cyclones which formed during the 2012-13 tropical cyclone season. This cyclone started forming on the 17th of January to the north of Queensland over the Gulf of Carpentaria (Figure 2.3). It continued to form over the sea, before crossing onto land at the Northern Territory/Queensland border and looping back out to sea by the evening of the 20th. During this period, the low pressure system was placed on watch, before being removed again once it made landfall as it was believed that the system would not progress into a tropical cyclone (BOM 2014). After returning to sea however, it once again increased in intensity, and on the 21st of January it was classified as a Category 1 cyclone and given its name just before making landfall slightly north of Kowanyama in northern Queensland on the same day (BOM 2013b).

Soon after making landfall, tropical Cyclone Oswald was downgraded to a tropical low, meaning the tropical cyclone was now ex-tropical Cyclone Oswald (BOM 2013b). Oswald's path continued in a more southward direction, following the eastern coast of Queensland

and New South Wales. Finally, the ex-tropical cyclone crossed back over the ocean to the south of Sydney on the 29th of January, seven days after its initial landfall as a cyclone (BOM 2013c). This was where the tropical low system finished, dissipating to the point where it was no longer considered a system, and the heavy rainfall decreased dramatically by the end of the month (BOM 2014).

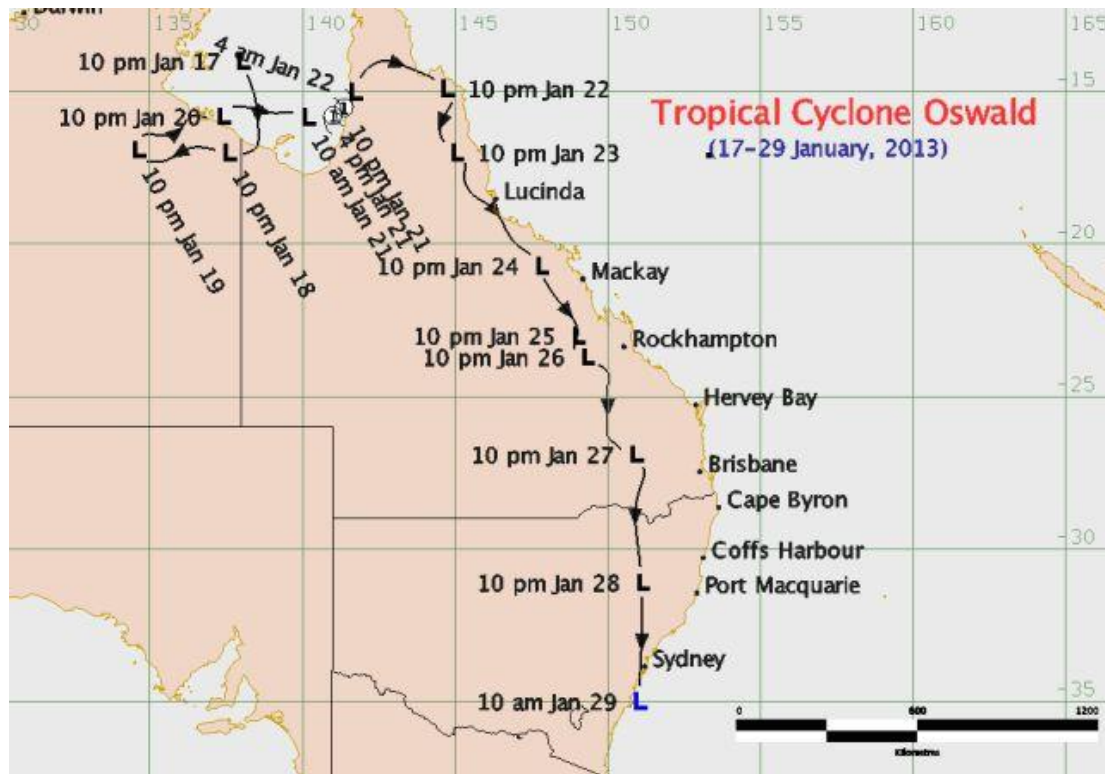


Figure 2.3 – Path of tropical Cyclone Oswald across the eastern side of Australia (Source: BOM 2013a)

During this time, tropical Cyclone Oswald broke a number of maximum rainfall records across eastern Queensland and New South Wales. Along the eastern coastline of the two states for the week ending the 29th of January 2013, the total rainfall was above 150mm, with some areas measuring a total amount of rainfall above 400mm (Figure 2.4). This coastline also experienced more than average amounts of rainfall for January 2013 (Figure

2.5), with the highest deviance from the average in this area occurring throughout south-east Queensland (BOM 2013b, 2013c).

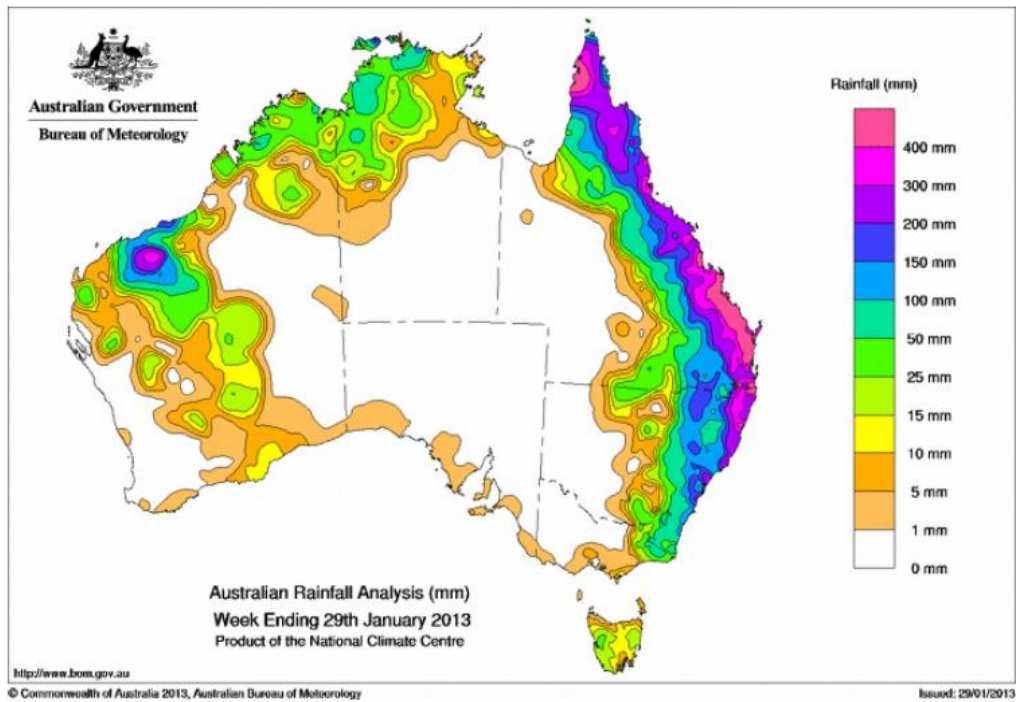


Figure 2.4 – Amount of rainfall for the week ending 29th January 2013 (Source: BOM 2013a)

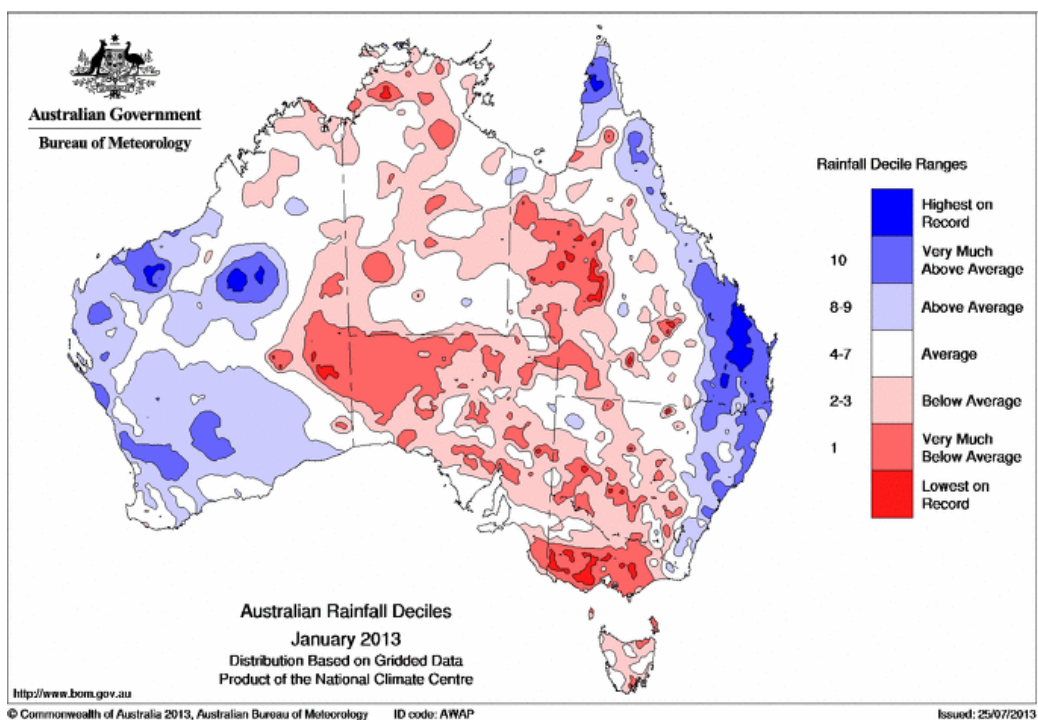


Figure 2.5 – The distribution of rainfall for January 2013. The blue sections indicate areas where the amount of rainfall was higher than average, and the red sections indicate the areas where rainfall was lower than average (Source: BOM 2014)

As a result, a number of flood events occurred across both states which lasted in some areas until the 17th of February 2013. The height of the flood waters also broke previous records at some locations. The most severe flooding occurring in the Burnett River and Laidley Creek in Queensland, and the Clarence River in New South Wales (BOM 2013b, 2013c).

In Queensland, there were also five confirmed reports of tornadoes, otherwise known as waterspouts. All five occurred in the Bundaberg region across approximately five hours on the afternoon of the 26th of January 2013. These tornadoes were caused by the severe thunderstorms that were present in the area, which were a result of ex-tropical Cyclone Oswald. Both the strong winds from these tornadoes as well as the tornadoes themselves resulted in a number of people becoming critically injured, while causing damage to property (BOM 2013b).

3 Data and Methodology

The following sections starts with an overview of the data which were used in this study.

This includes tide gauge data, satellite altimetry data, rainfall data and stream discharge data. An explanation of each dataset is given, covering what the data are and where they were collected. The next section then explains the multivariate regression model and the process involved.

3.1 Data

3.1.1 SSH - Tide Gauge

The SSHs measured by tide gauges was utilised from the University of Hawaii Sea Level Centre (UHSLC) (<http://uhslc.soest.hawaii.edu/data/>) and the Queensland Government Datasets (<https://data.qld.gov.au/dataset>). The data from UHSLC was presented in hourly measurements in millimetres, then converted to metres for the modelling. The Queensland Government data, in metres, were averaged to hourly increments as these were presented in ten minute intervals.

In total, nineteen tide gauge data sets were used (Table 3.1), taken from sixteen locations (Figure 3.1). From this point forward, the data used has been presented per location, as there are two tide gauges in some locations. This is because SSH data collected from newer tide gauges have been recorded as a continuation of the data from the older tide gauge.

These sets were chosen as SSH data were measured at the sixteen locations around the period and track of tropical Cyclone Oswald from the 15th of January to the 15th of February 2013. All sixteen data sets were used to describe SSH during Oswald, by graphing the data in Microsoft Excel. Three of the tide gauges were then chosen for the model –

Burnett Heads, Rosslyn Bay, and Urangan. This was based on their proximity to Hervey Bay

(Figure 3.1).

Table 3.1 – Information about selected tide gauges (Sources: UHSLC (<http://uhslc.soest.hawaii.edu/data>) and Queensland Government Datasets (<https://data.qld.gov.au/dataset/>))

Station	Name	Source	Latitude	Longitude	Time Period
062	Darwin	UHSLC	12.5°S	130.9°E	01/01/1983 to 31/07/2016
071004A	Karumba Storm Surge	QLD Government	17.5°S	140.8°E	01/01/1996 to 31/12/2015
070021A	Weipa Storm Surge	QLD Government	12.7°S	141.9°E	01/01/1996 to 31/12/2015
056012A	Cairns Storm Surge	QLD Government	17.0°S	145.8°E	01/01/1996 to 31/12/2008
100280	Cairns Storm Surge No 7 Wharf	QLD Government	16.9°S	145.8°E	01/01/2009 to 31/12/2015
063012A	Mourilyan Storm Surge	QLD Government	17.6°S	146.1°E	01/01/1996 to 31/12/2015
055003A	Townsville Storm Surge	QLD Government	19.3°S	146.8°E	01/01/1996 to 25/09/2011
100447	Townsville Berth 1 Pumphouse	QLD Government	19.3°S	146.8°E	26/09/2011 to 31/12/2015
061007A	Bowen Storm Surge	QLD Government	20.0°S	148.3°E	01/01/1996 to 31/12/2015
030003A	Shute Harbour Storm Surge	QLD Government	20.3°S	148.8°E	01/01/1996 to 31/12/2015
054004A	Mackay Storm Surge	QLD Government	21.1°S	149.2°E	01/01/1996 to 31/12/2006
100084	Mackay Outer Harbour Storm Surge	QLD Government	21.1°S	149.2°E	01/01/2007 to 31/12/2015
024011A	Rosslyn Bay	QLD Government	23.2°S	150.8°E	04/12/2001 to 31/12/2015
050008A	Port Alma Storm Surge	QLD Government	23.6°S	150.9°E	01/01/1996 to 31/12/2015
052027A	Gladstone Auckland Point	QLD Government	23.8°S	151.3°E	01/01/1996 to 31/12/2015
059	Burnett Heads (Bundaberg)	UHSLC	24.8°S	152.4°E	01/01/1984 to 31/07/2016
058009B	Urangan Storm Surge	QLD Government	25.3°S	152.9°E	01/01/1996 to 31/12/2015
011008A	Mooloolaba Storm Surge	QLD Government	26.7°S	153.1°E	01/01/1996 to 31/12/2015
057	Fort Denison (Sydney)	UHSLC	33.9°S	151.2°E	01/01/1965 to 31/07/2016

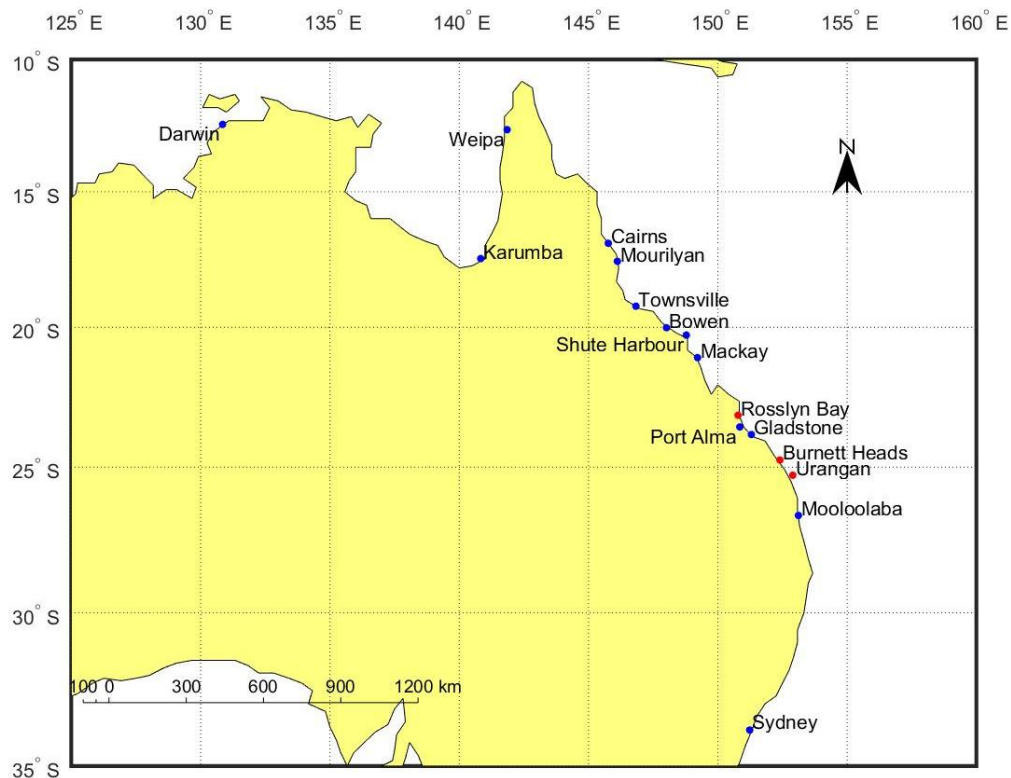


Figure 3.1 – Locations of tide gauges. The red points represent the three tide gauges used for the model and validation (Sources: UHSLC (<http://uhslc.soest.hawaii.edu/data>) and Queensland Government Datasets (<https://data.qld.gov.au/dataset/>))

3.1.2 SSH - Satellite Altimeters

The SSHs measured by satellite altimeters was utilised from the Radar Altimetry Database (RADS) (<http://rads.tudelft.nl/rads/rads.shtml>), and consisted of data collected during the TOPEX/Poseidon (1992 to 2003), Jason-1 (2001 to 2013) and Jason-2 (2008 to 2016, still in commission) missions every ten days.

For the model, data measured in the area 15°S to 30°S and 145°E to 160°E were used (Figure 3.2). The data were measured between August 1992 and December 2014. This area was chosen to cover the majority of the Queensland coastline.

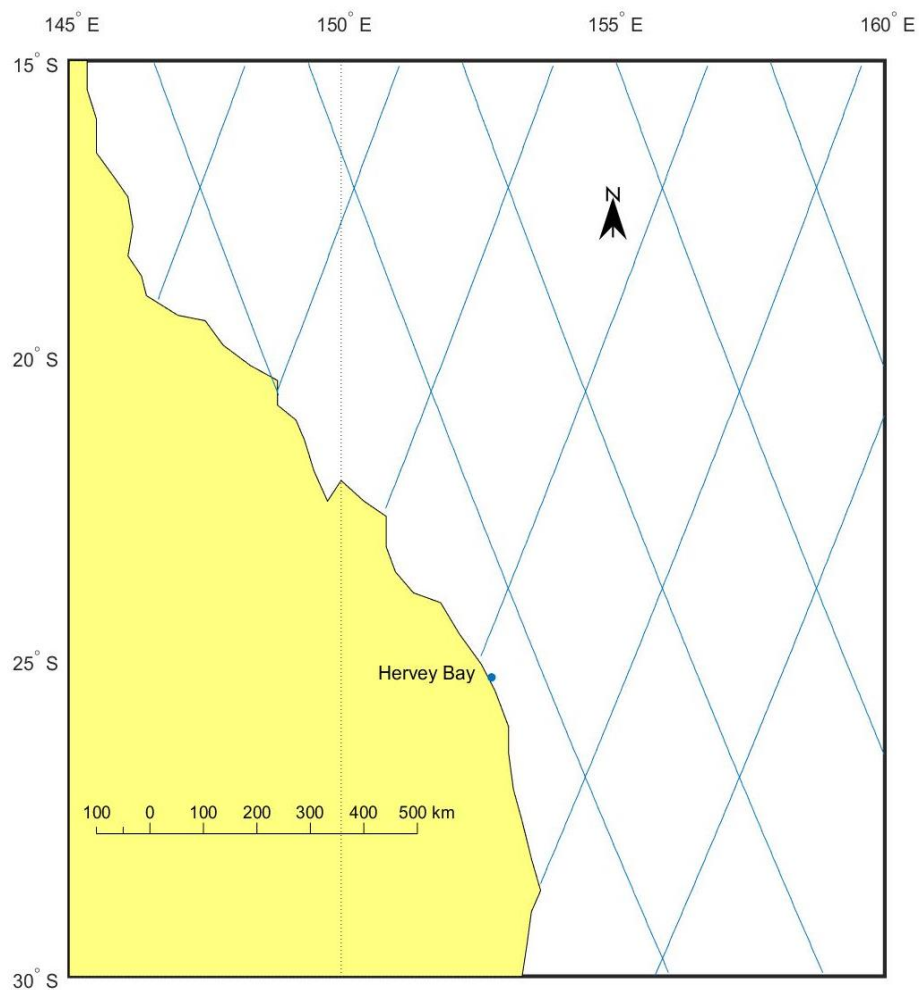


Figure 3.2 – Locations of the data collected by the satellite altimeter tracks around Queensland, shown as the blue lines (Source: RADS (<http://rads.tudelft.nl/rads/rads.shtml>))

3.1.3 Rainfall Data

Rainfall data were derived from the Bureau of Meteorology Climate Data

(<http://www.bom.gov.au/climate/data/>). These data are measured by rain gauges in millimetres, and collected either through manual readings or automated systems.

Recording occurs at 9:00 AM local time each morning, giving the total amount of rainfall for the past twenty-four hours.

To describe the effect of tropical cyclone Oswald on rainfall patterns, 15 recording stations were selected (Figure 3.3, Table 3.2). These stations were selected as the location of each of the rainfall measuring stations were the closest to the tide gauges selected above, and were within 15km of the tide gauge. All data were graphed in Microsoft Excel, from the 15th of January to the 15th of February 2013.

Table 3.2 – Information about selected rainfall measuring stations (Source: Bureau of Meteorology Climate Data (<http://www.bom.gov.au/climate/data/>))

Station	Name	Latitude	Longitude	Time Period
14167	Stokes Hill	12.46°S	130.85°E	01/01/1968 to 23/10/2016
29063	Normanton Airport	17.69°S	141.07°E	11/04/2001 to 23/10/2016
27042	Weipa Eastern Ave	12.63°S	141.88°E	01/01/1914 to 16/10/2016
31218	Parramatta Park	16.91°S	145.76°E	01/06/2001 to 30/09/2016
32037	South Johnstone Exp Stn	17.61°S	146°E	01/01/1920 to 23/10/2016
32040	Townsville Aero	19.25°S	146.77°E	01/01/1941 to 23/10/2016
33268	Reeves Alert	20.15°S	148.16°E	30/11/2000 to 15/09/2016
33017	Daydream Island Resort	20.26°S	148.81°E	01/01/1949 to 31/10/2013
33303	Mackay Alert	21.14°S	149.19°E	15/12/2000 to 23/10/2016
39344	Darts Creek	23.74°S	150.94°E	01/08/2011 to 30/09/2016
39123	Gladstone Radar	23.86°S	151.26°E	01/12/1957 to 23/10/2016
39135	Bargara	24.8°S	152.45°E	01/07/1926 to 03/09/2013
40405	Hervey Bay Airport	25.32°S	152.88°E	12/03/1999 to 23/10/2016
40861	Sunshine Coast Airport	26.6°S	153.09°E	07/07/1994 to 23/10/2016
66006	Sydney Botanic Gardens	33.87°S	151.22°E	01/01/1885 to 13/10/2016

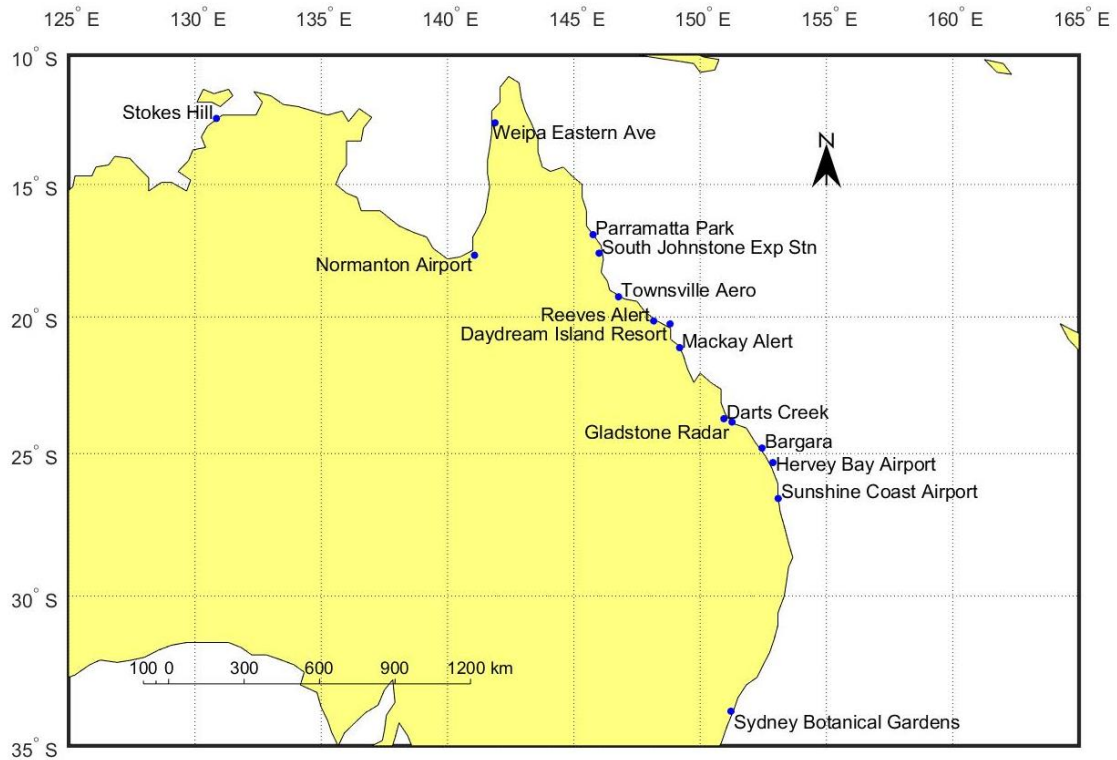


Figure 3.3 – Locations of selected rainfall measuring stations (Source: Bureau of Meteorology Climate Data (<http://www.bom.gov.au/climate/data/>))

3.1.4 Stream Discharge Data

Stream discharge data were utilised from the Queensland Government’s Water Monitoring Information Portal (<https://water-monitoring.information.qld.gov.au/>). These data were measured at stream and river monitoring sites approximately every thirty minutes. For the plotting, the data used were daily totals in ML/day.

Eight stations in total were selected to show what occurred during tropical Cyclone Oswald (Figure 3.4, Table 3.3). These stations were select as they were located on a flowing body of water which reaches the ocean near a tide gauge. All data were graphed in Microsoft Excel, from the 15th of January to the 15th of February 2013.

Table 3.3 – Information about selected stream discharge measuring stations (Source: Queensland Government’s Water Monitoring Information Portal (<https://water-monitoring.information.qld.gov.au/>))

Station	Name	Latitude	Longitude	Time Period
916001B	Norman River at Glenore Weir	17.9°S	141.1°E	07/12/1974 to 23/10/2016
110001D	Barron River at Myola	16.8°S	145.6°E	01/10/1982 to 23/10/2016
112004A	North Johnstone River at Tung Oil	17.6°S	145.9°E	01/10/1966 to 23/10/2016
121003A	Don River at Reeves	20.1°S	148.2°E	14/03/1984 to 23/10/2016
125016A	Pioneer River at Dumbleton Weir T/W	21.1°S	149.1°E	22/12/2005 to 23/10/2016
130005A	Fitzroy River at The Gap	23.1°S	150.1°E	30/04/1964 to 23/10/2016
136007A	Burnett River at Figtree Creek	25.3°S	152.0°E	22/01/1997 to 23/10/2016
138014A	Mary River at Home Park	25.8°S	152.5°E	29/06/1982 to 23/10/2016

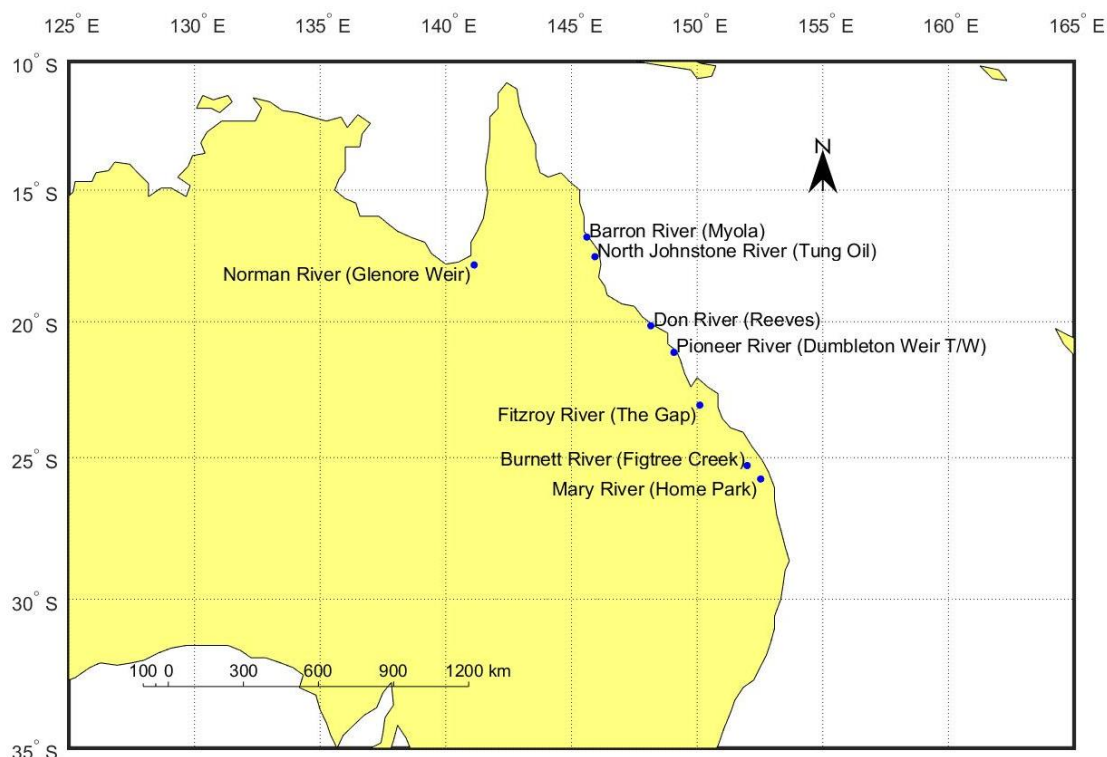


Figure 3.4 – Locations of stream discharge measurement stations. The names consist of the river the station is on and the name of the station in brackets (Source: Queensland Government’s Water Monitoring Information Portal (<https://water-monitoring.information.qld.gov.au/>))

3.2 Method

In order to predict changes in SSH during a tropical cyclone, a model is required. A number of researchers have utilised the hydrodynamic model for this, including Haigh et al. (2013) and Madsen et al. (2015). The model used here, however, was the multivariate regression model (Høyer & Andersen 2003):

$$\vec{y} = \mathbf{X} \cdot \vec{b} + \vec{\varepsilon} \quad [1]$$

where y is a vector of satellite altimetry data, X is a matrix of tide gauge data, b is a vector of coefficients and ε is a vector of prediction error. This model was chosen due to being successfully used by Deng et al. (2015) and Høyer and Andersen (2003). The coding for this model in MATLAB, which was also used by Deng et al. (2015), was also readily available. This was supplied by Z Gharineiat (2016, pers comm., 28 Jul).

Before the model could be run, the tide levels needed to be removed from the SSH data to give comparable sea level anomalies (SLAs). This was completed so a relationship between SSH data measured by tide gauges and satellite altimeters could be established. For this, the response method was used, which utilises both the harmonic analysis and the least squares adjustment (as demonstrated by Munk & Cartwright 1966). The use of this method on SSH data from tide gauges and satellite altimeters is shown in the research completed by Gharineiat and Deng (2015). For this dissertation, this adjustment to the data was completed by Z Gharineiat (2016, pers comm., 28 Jul).

Once the SLAs were collected, the multivariate regression model was then applied (Equation 1). Firstly, b had to be calculated. The time at which the altimetry SLA data were collected was compared to the tide gauge SLA data collection times. Each of the tide gauge SLA data points from the selected tide gauges which were close were then averaged with the three

hours of data either side of this point. The altimetry data and the averaged tide gauge data were then used to calculate b . This was through the use of the least squares adjustment, in order to minimise the error (Høyer & Andersen 2003):

$$\vec{b} = (\mathbf{X}^T \mathbf{X})^{-1} \mathbf{X}^T \vec{y} \quad [2]$$

Once calculated, b was then placed in the model along with the hourly tide gauge SLA data to calculate the hourly altimetry SLA. The correlation between the predicted and measured SLAs by satellite altimeters was then calculated, to see how well the predicted data fitted the measured data.

To describe how well the model performed, two different, independent methods were used, following the method of Deng et al. (2015). The first was the hindcast skill (R^2) (Emery & Thomson 2001):

$$R^2 = \frac{\sum (y_i - \bar{y})^2 - \sum (y_i - \hat{y}_i)^2}{\sum (y_i - \bar{y})^2} \quad [3]$$

where y_i represents each of the measured satellite data points, \bar{y} is the mean of the measured values, and \hat{y}_i is each of the estimated satellite data which was predicted through the model (Equation 1). An R^2 value closer to one indicates the model performed well.

The other method was the root mean square error (RMSE) (Høyer & Andersen 2003):

$$RMS_e = \sqrt{(\varepsilon^2)} \quad [4]$$

where values closer to zero indicate the model performed well.

Once the modelling was completed, the model was then validated. This was completed by using the calculated b values to predict the SLAs at a tide gauge which was not used in the

initial modelling. These values were plotted against the measured SLA values at Urangan.

The Urangan SLA data were calculated by removing tide levels from the SSH data.

In total, this entire process was completed twice. The first time, only one set of tide gauge data was used (Burnett Heads). The second time, two sets tide gauge data were used (Burnett Heads and Rosslyn Bay). This was done to see whether the use of one or two sets of SLA data would give better predictions.

4 Results

In this section, the results which were found from using the methods above have been presented. Firstly, the tide gauge, rainfall and stream discharge data which was measured is presented. This is to show what occurred during tropical Cyclone Oswald, particularly along the Queensland coastline. The results from the modelling are then presented.

4.1 Tropical Cyclone Oswald

4.1.1 Tide Gauge Data

From the tide gauge locations which were chosen, all 16 recorded data across the month to show what occurred (Figure 4.1). This data is presented as the daily average SSH.

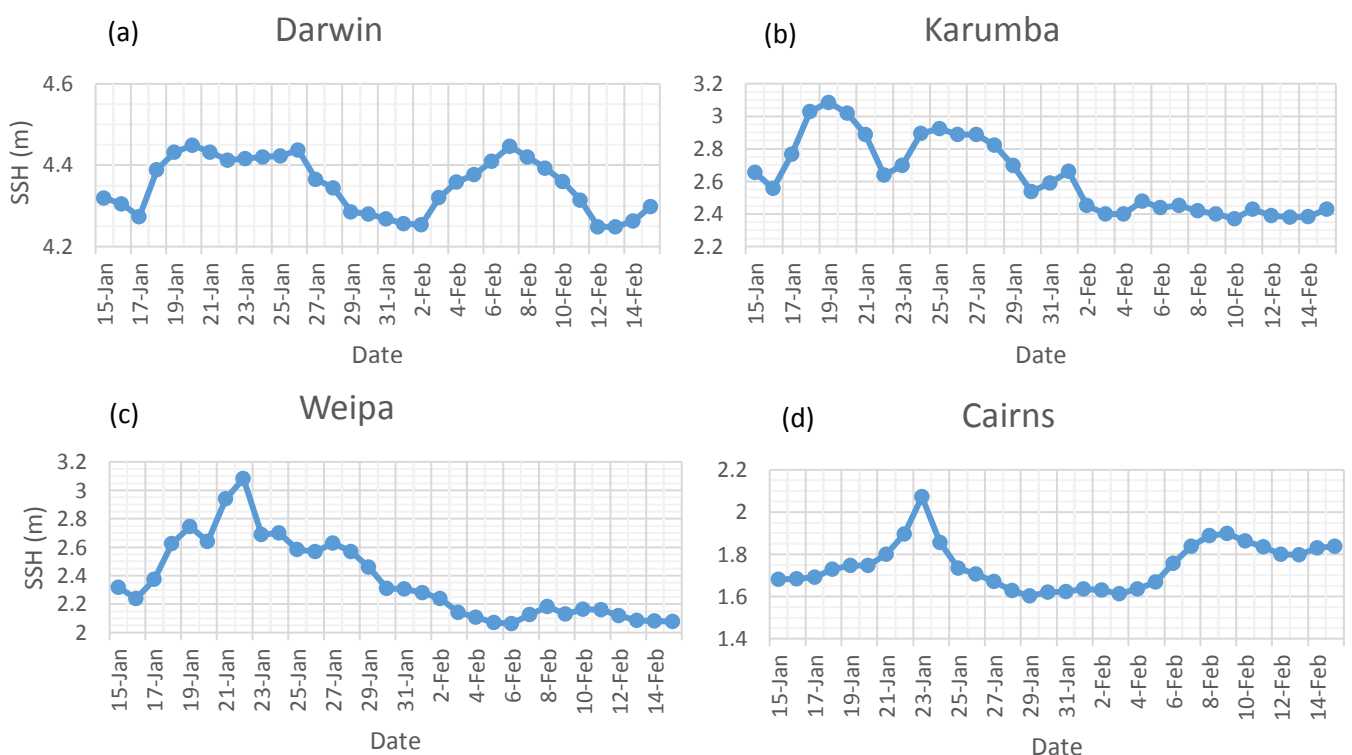


Figure 4-1 - Daily mean SSH in metres, measured by tide gauges during tropical Cyclone Oswald. Any days which did not have a full day of data were not included. Graphs are ordered in terms of their positioning along the coastline, starting from Darwin and moving to the right. The y-axis is not in the same range across the graphs, however, the increments of the axis have been kept the same for comparison (Sources: UHSLC (<http://uhslc.soest.hawaii.edu/data>) and Queensland Government Datasets (<https://data.qld.gov.au/dataset/>))

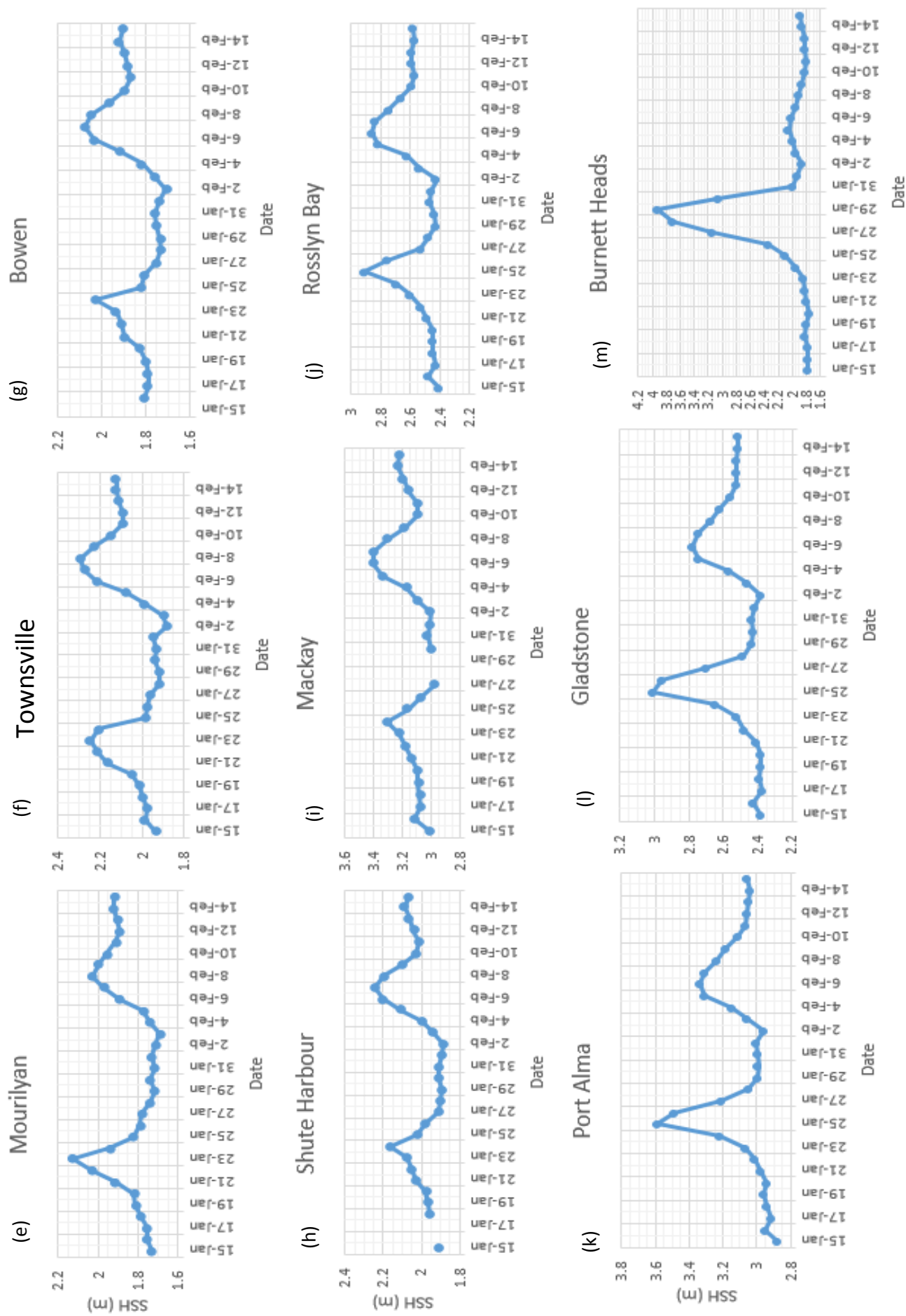


Figure 4-1 - Daily mean SSH in metres, measured by tide gauges during tropical Cyclone Oswald. Any days which did not have a full day of data were not included. Graphs are ordered in terms of their positioning along the coastline from Darwin and moving to the right. The y-axis is not in the same range across the graphs, however, the increments of the axis have been kept the same for comparison (Sources: UHSLC (<http://uhslc.soest.hawaii.edu/data>) and Queensland Government Datasets (<https://data.qld.gov.au/dataset>)).

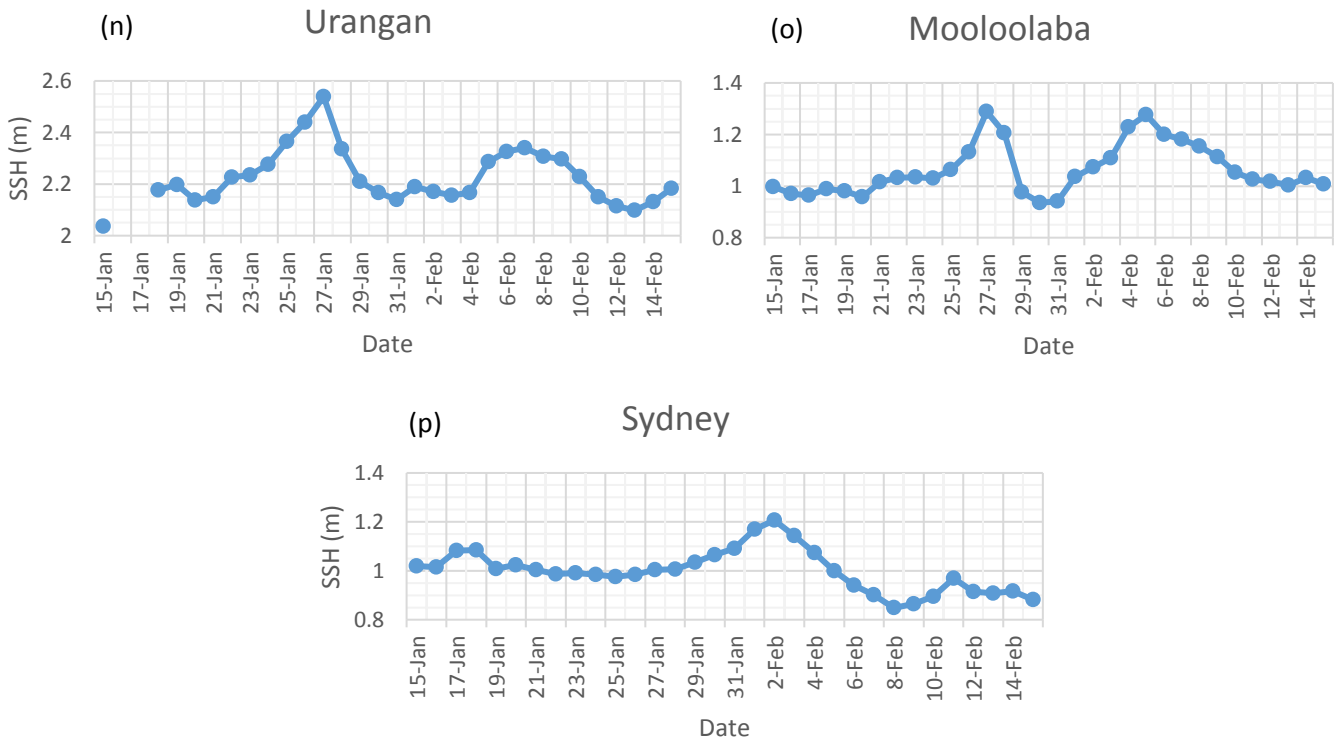


Figure 4-1 - Daily mean SSH in metres, measured by tide gauges during tropical Cyclone Oswald. Any days which did not have a full day of data were not included. Graphs are ordered in terms of their positioning along the coastline, starting from Darwin and moving to the right. The y-axis is not in the same range across the graphs, however, the increments of the axis have been kept the same for comparison (Sources: UHSLC (<http://uhslc.soest.hawaii.edu/data>) and Queensland Government Datasets (<https://data.qld.gov.au/dataset>))

Across all 16 tide gauge locations, there was a change in SSH either during or just after tropical Cyclone Oswald had passed the area. This was followed by another, smaller increase occurring days later, which was due to the amount of water still in the area after the cyclone. The largest difference between the maximum and minimum SSH occurred at the Burnett Heads tide gauge, with a difference of approximately 2.2 m. The highest SSH occurred around the 29th of January.

The smallest difference between the maximum and minimum SSH was measured by the Darwin tide gauge, with a difference of approximately 0.2 m. This was due to Cyclone Oswald only showing the characteristics of a tropical low when it was close to Darwin, and was losing strength as it was over land.

4.1.2 Rainfall Data

The measurements from all 15 rainfall stations were graphed (Figure 4.2). This data is presented as the daily total rainfall.

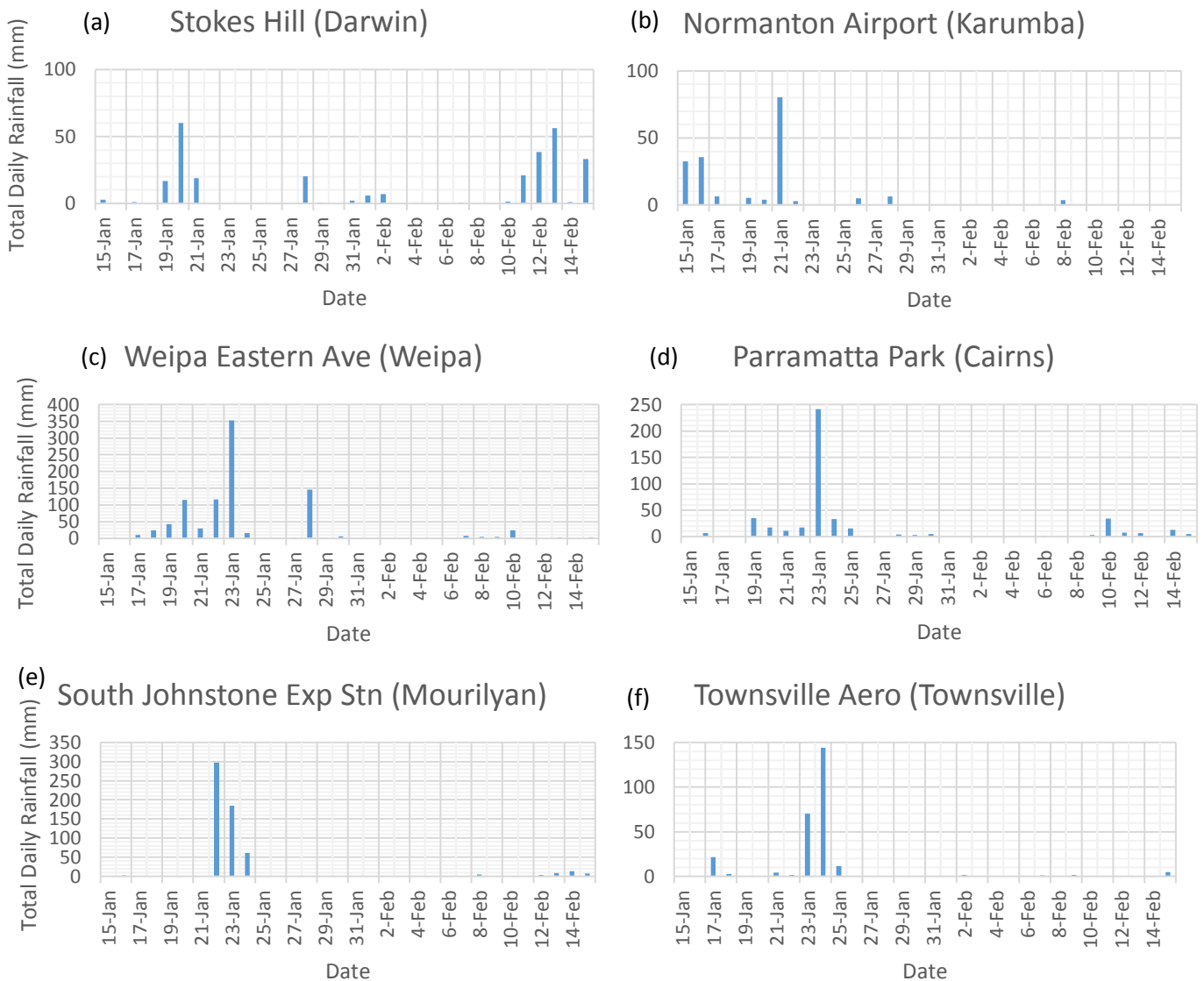


Figure 4-2 – Daily total rainfall in millimetres, measured during tropical Cyclone Oswald. Any measurements which contain more than one day’s worth of data have not been included. The graphs are ordered in terms of their positioning along the coastline, starting from Stokes Hill and moving to the right. The y-axis across the graphs are not the same range, but they all are in increments of 50 mm to help with the comparison (Source: Bureau of Meteorology Climate Data (<http://www.bom.gov.au/climate/data/>))

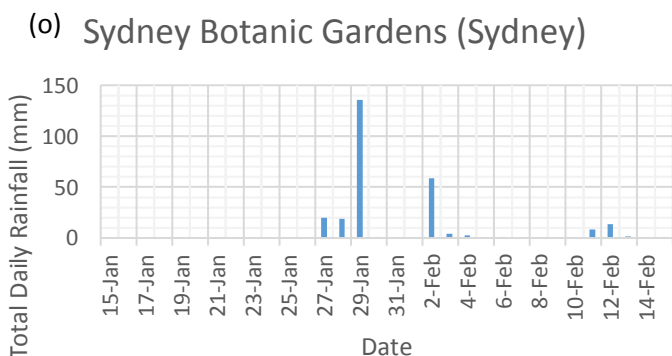
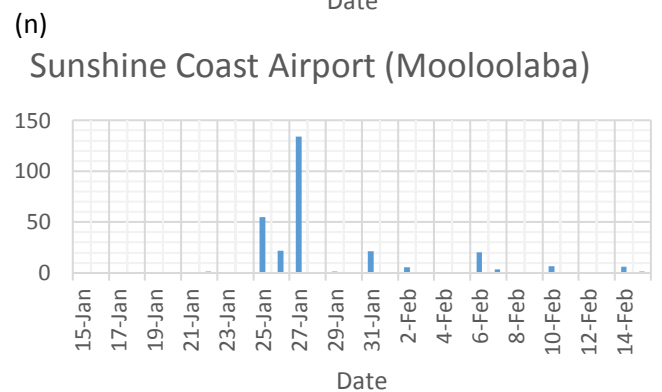
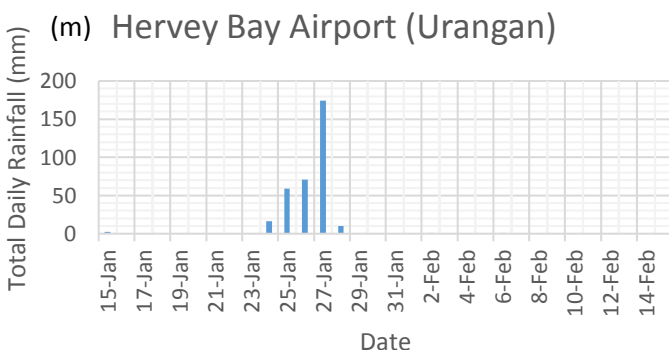
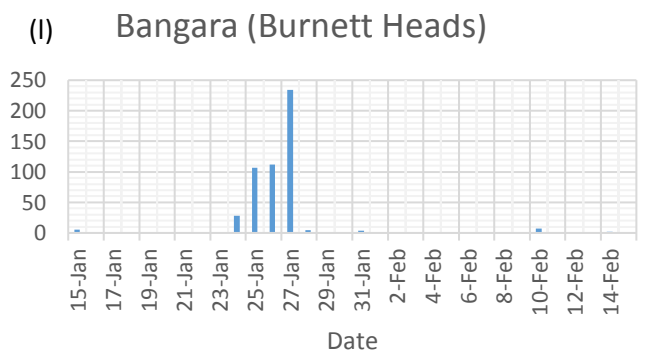
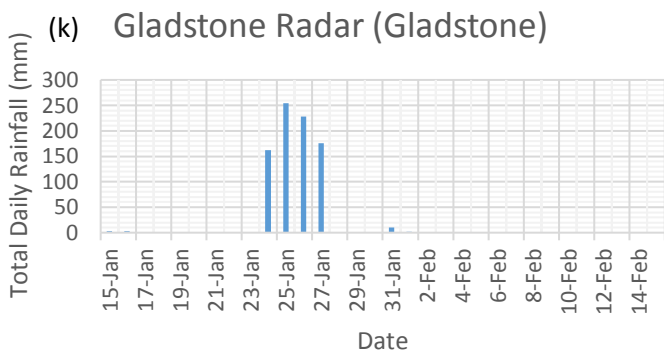
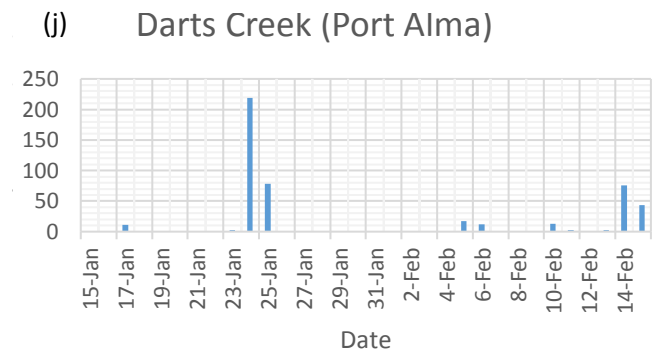
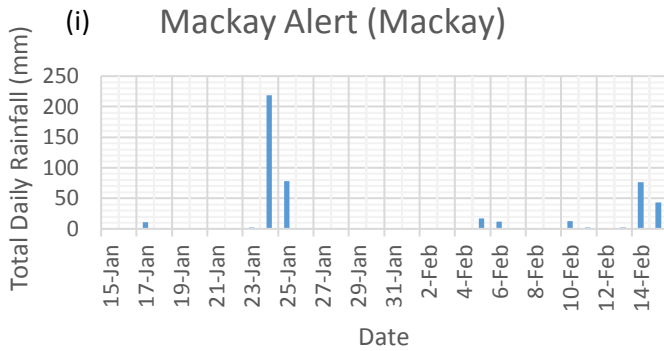
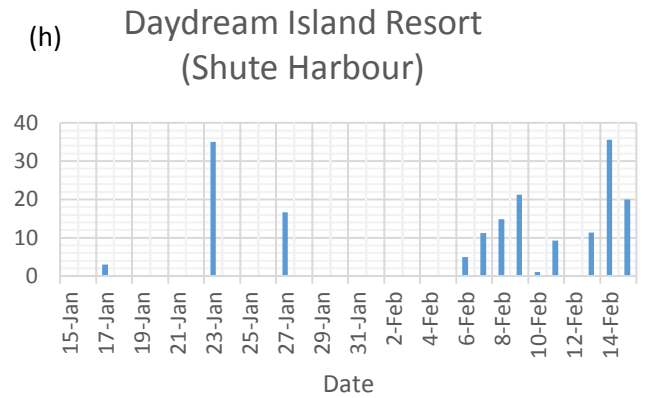
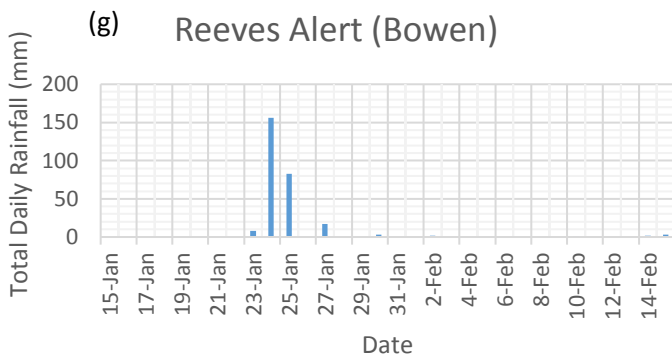


Figure 4-2 – Daily total rainfall in millimetres, measured during tropical Cyclone Oswald. Any measurements which contain more than one day's worth of data have not been included. The graphs are ordered in terms of their positioning along the coastline, starting from Stokes Hill and moving to the right. The y-axis across the graphs are not the same range, but they all are in increments of 50mm to help with the comparison (Source: Bureau of Meteorology Climate Data (<http://www.bom.gov.au/climate/data/>))

The 15 rainfall measuring stations chosen all recorded the maximum daily total rainfall during the month when tropical Cyclone Oswald was passing through or near the station. The daily totals either side of the maximum were significantly smaller across the board. For five of the stations, the maximum daily total equalled more than half of the total for the month – Parramatta Park (241 mm 23/01/13, 460.4 mm total), Townsville Aero (144.2 mm 24/01/13, 265.8 mm total), Reeves Alert (156 mm 24/01/13, 275 mm total), Hervey Bay Airport (174.4 mm 27/01/13, 336.8 mm total) and Sydney Botanic Gardens (135.8 mm 29/01/13, 267.1 mm total).

Weipa Eastern Ave recorded the highest daily rainfall amount at approximately 352mm on the 23rd of January 2013. This station also recorded the largest amount of rainfall across the month, with approximately 908mm recorded. This was due to the path Oswald took. After crossing onto land as a Category 1 tropical cyclone, Oswald travelled north-east. This meant that Weipa Eastern Ave experienced the rainfall of a Category 1 cyclone, while the cyclone also stayed within the vicinity of the station for almost two days.

Although Normanton Airport was the closest station when Oswald was a Category 1 and made landfall, it was the station which recorded the least amount of rainfall during the month. In total, approximately 182 mm was recorded, with the highest amount of approximately 80 mm occurring on the 21st of January 2013. This was the day Oswald made landfall.

4.1.3 Stream Discharge Data

From the selected recording stations, all eight were graphed (Figure 4.3). The graphs are in ML/day.

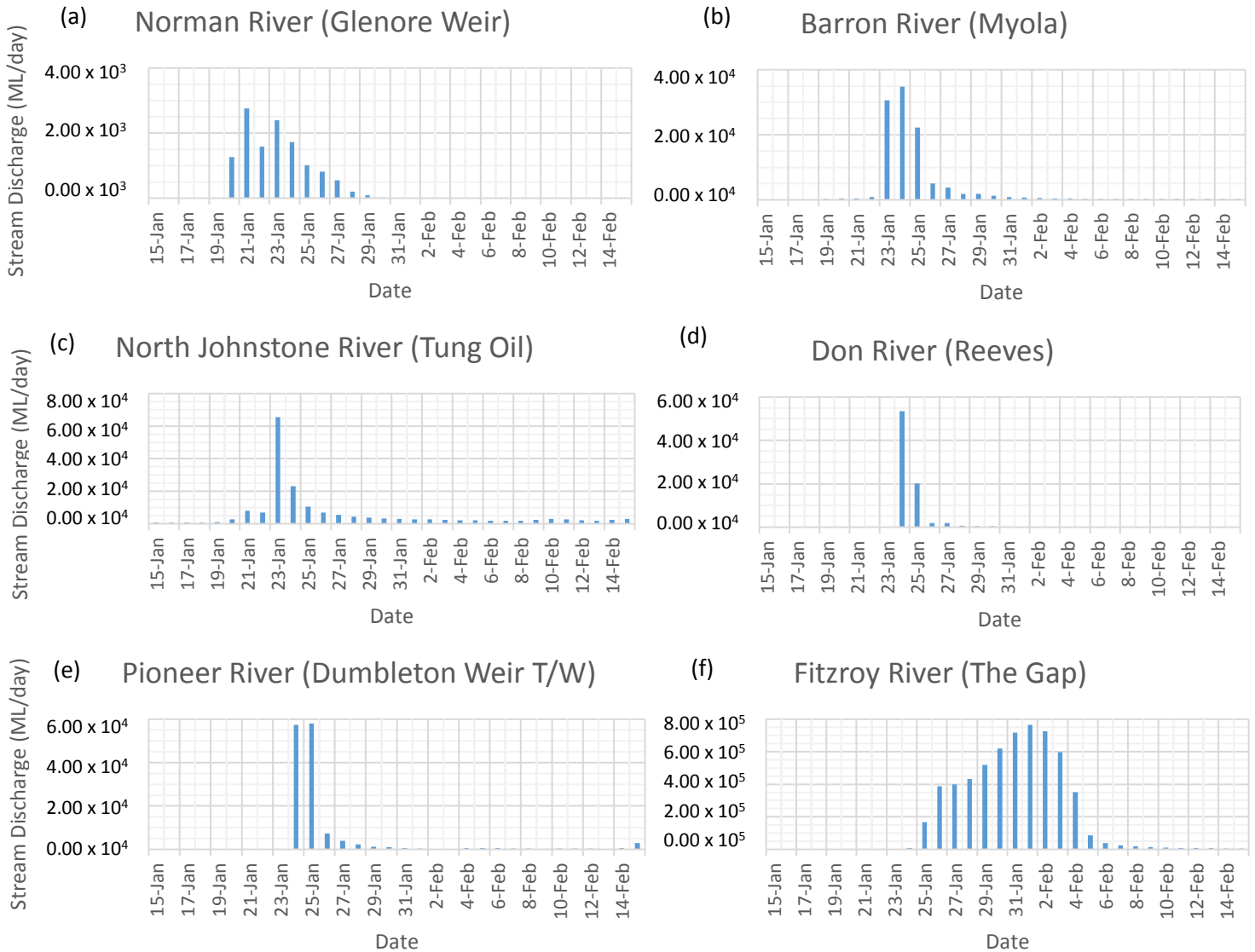


Figure 4-3 - Daily total stream discharge in megalitres per day, measured during tropical Cyclone Oswald. They are ordered in terms of their positioning along the coastline, starting from Norman River (Glenore Weir) and moving to the right. The y-axis across the graphs are not the same range (Source: Queensland Government's Water Monitoring Information Portal (<https://water-monitoring.information.qld.gov.au/>))

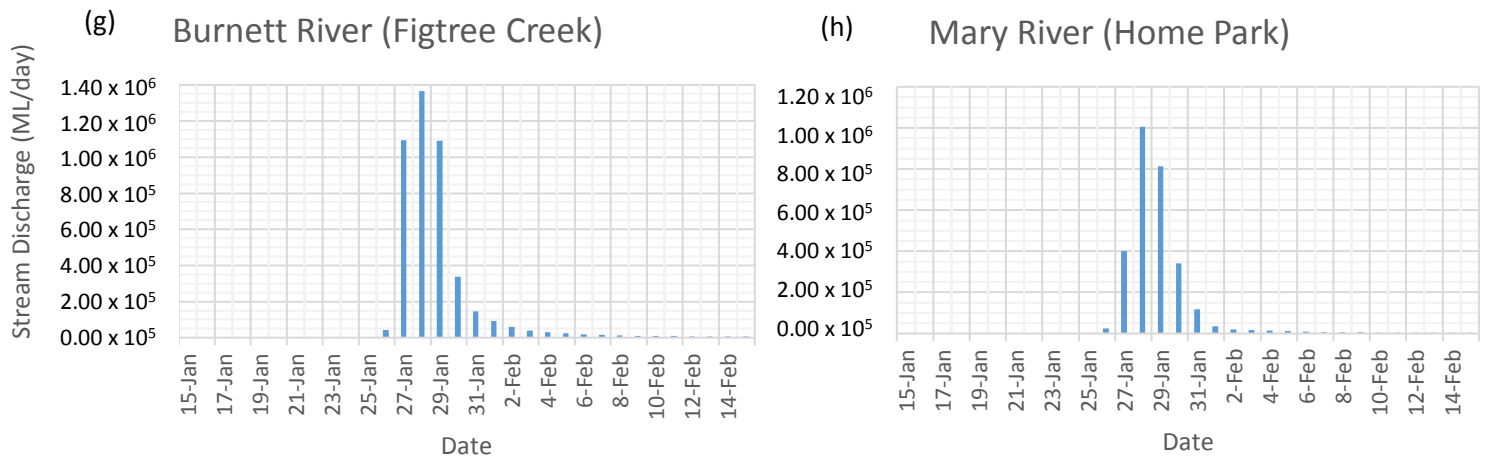


Figure 4-3 - Daily total stream discharge in megalitres per day, measured during tropical Cyclone Oswald. They are ordered in terms of their positioning along the coastline, starting from Norman River (Glenore Weir) and moving to the right. The y-axis across the graphs are not the same range (Source: Queensland Government's Water Monitoring Information Portal (<https://water-monitoring.information.qld.gov.au/>))

During the course of tropical Cyclone Oswald, all recorded peaks occurred as the cyclone passed through the area. Also, the recorded maximum daily discharge for the month generally increased from one area to the next. The main factors which would influence this include the strength of the cyclone, the amount of rainfall in the area during the period, and the amount of water the rivers were able to hold.

Out of all the locations, only one measured its peak daily total to be more than half of the monthly total. This was Don River (Reeves) (5.34×10^4 ML/day 24/01/13, 8.04×10^4 ML/day total). The largest daily discharge was measured at Burnett River (Figtree Creek), with an amount of approximately 1.37×10^6 ML/day recorded on the 28th of January. This large amount of discharge shows one of the reasons why the Burnett River flooded. The largest total discharge for the month was recorded at Fitzroy River (The Gap), with a total of approximately 5.92×10^6 ML/day. The Fitzroy River system is located around where Oswald stalled, so a larger amount of rainfall would have occurred in the area.

The smallest total discharge for the month was recorded at Norman River (Glenore Weir) at approximately 1.24×10^4 ML/day. The path Oswald took did not cross over the Norman River, and was only around the area as a tropical low. Also, when landfall occurred Oswald moved away from the river system. This would have resulted in less water being collected in the system.

4.2 Multivariate Regression Model

4.2.1 Distribution of Temporal Correlation Coefficients

Firstly, the correlation between the measured and predicted satellite altimetry SLA data was calculated and plotted, to show how well the predicted data fitted the measured data. The predicted SLA, along with the correlation between the data measured by tide gauges and satellite altimeters, has been presented for one tide gauge (Figure 4.4), then two tide gauges (Figure 4.5).

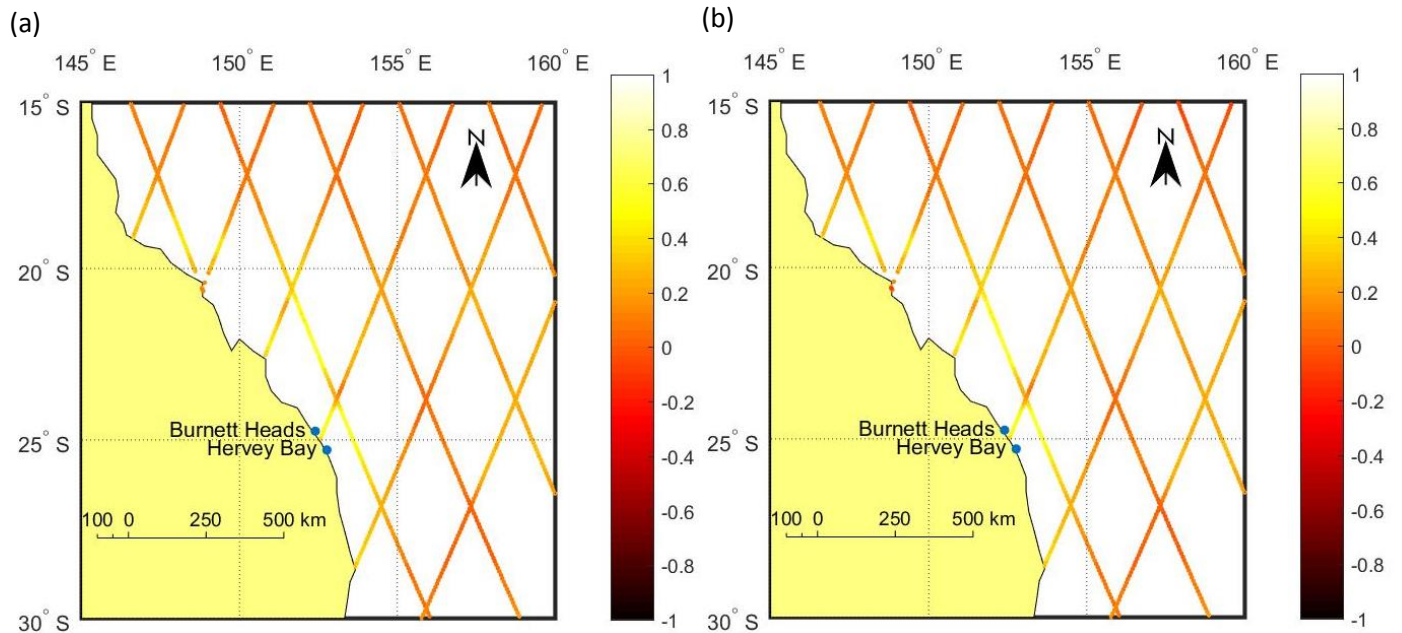


Figure 4.4 – Distribution of temporal correlation coefficients (Burnett Heads only) – (a) predicted and (b) measured

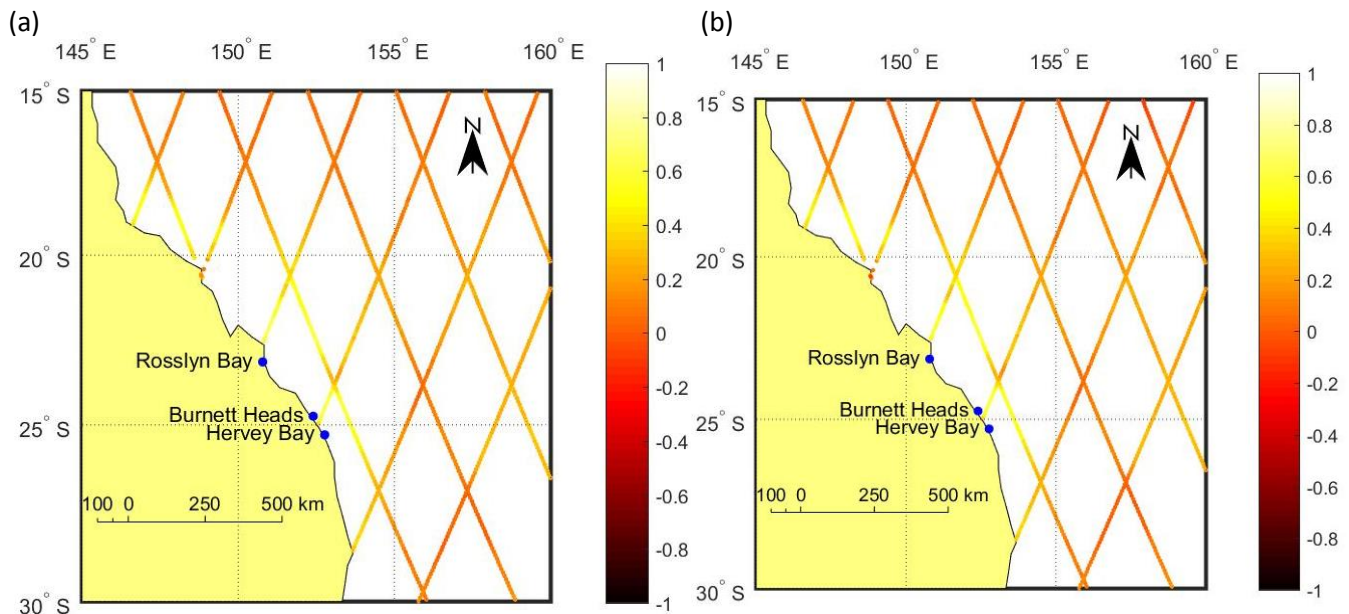


Figure 4.5 – Distribution of temporal correlation coefficients (Burnett Heads and Rosslyn Bay) – (a) predicted and (b) measured

Around the area where the Burnett Heads tide gauge is located, the correlation was approximately 0.6. This extended along the coastline to the north, with areas as far as Mourilyan and Cairns also showing a correlation around 0.6. Further away from the coast, the correlation was closer to 0.2. There was then a gradual increase in correlation moving towards the coastline.

When both Burnett Heads and Rosslyn Bay SLA data was used in the model, the best correlation was at approximately 0.65. This occurred within the immediate vicinity of both the tide gauges. Other coastal area stayed at around 0.6, and the area which had this correlation increased. Even in small increments, the overall correlation increased slightly between this output and that of the one tide gauge output.

For both of the runs of the model, the correlation of the predicted SLA was the same as the correlation of the measured SLA. The values which were achieved from the model were therefore as good as they could be, as the correlation of the predicted values can only be as high as the measured data. Also, even though the values were the same, the measured data

by itself cannot be used to predict values at a certain point. This is because the relationship between the measured SLA by the tide gauges and the measured SLA by the satellite altimeters has not been established.

4.2.2 Tests of Performance

How well the model performed was then tested. This was through the calculation of the RMS ϵ (Figure 4.6) and the use of the hindcast skill (Figure 4.7). The results when using one set of SLA data from one tide gauge and two sets of SLA data from two tide gauges has been plotted.

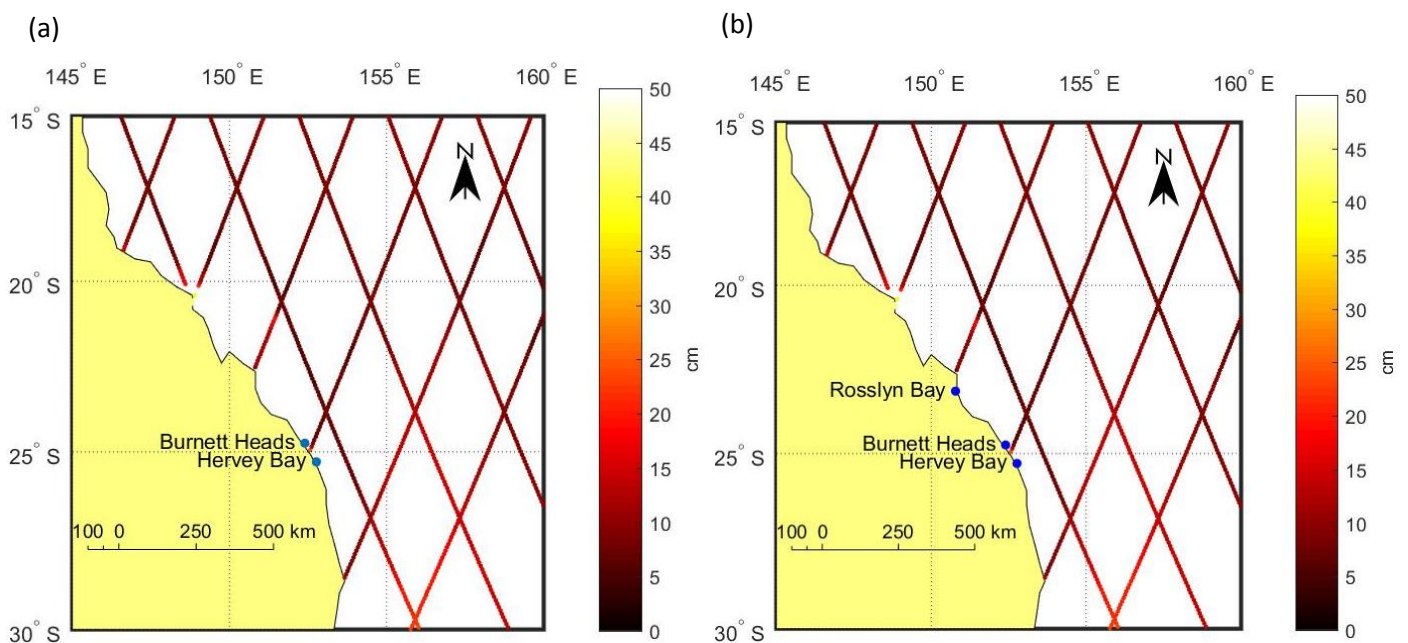


Figure 4.6 – RMS ϵ - (a) Burnett Heads only and (b) Burnett Heads and Rosslyn Bay

The RMS ϵ using only Burnett Heads SLA data showed that the model performed fairly well around the location of the tide gauge. The values around the general area of the tide gauges were approximately six. The points closest to the coastline were then around twenty, with a small area further north along the coast from Rosslyn Bay sitting close to forty. This means the model did not perform as well directly along the coast, either due to shallow-water

gravity anomalies or the tide gauges not fully representing what was occurring all the way along the coastline.

Overall, the RMS ϵ across the area was between approximately six and ten. The performance of the model to the south of the tide gauge was a lot poorer, with values around the twenty mark. This shows, like the coastline, that the model did not perform as well in this area either.

The RMS ϵ results were improved when using two sets of SLA data (Burnett Heads and Rosslyn Bay). This improvement was only slight however, and occurred mainly around the location of the additional tide gauge, Rosslyn Bay. Across the area, the RMS ϵ was between six and ten, with both the values along the coastline and to the south of the tide gauges being around the twenties. Again, there was also a small area further north along the coast from Rosslyn Bay sitting close to forty.

The improvement through the second RMS ϵ values meant that using two sets of SSH data resulted in a better performance of the model compared to using one set. Even with this improvement, however, the best scenario would be for the RMS ϵ to be close to zero. This means that the performance of both runs was not as good as it could have been.

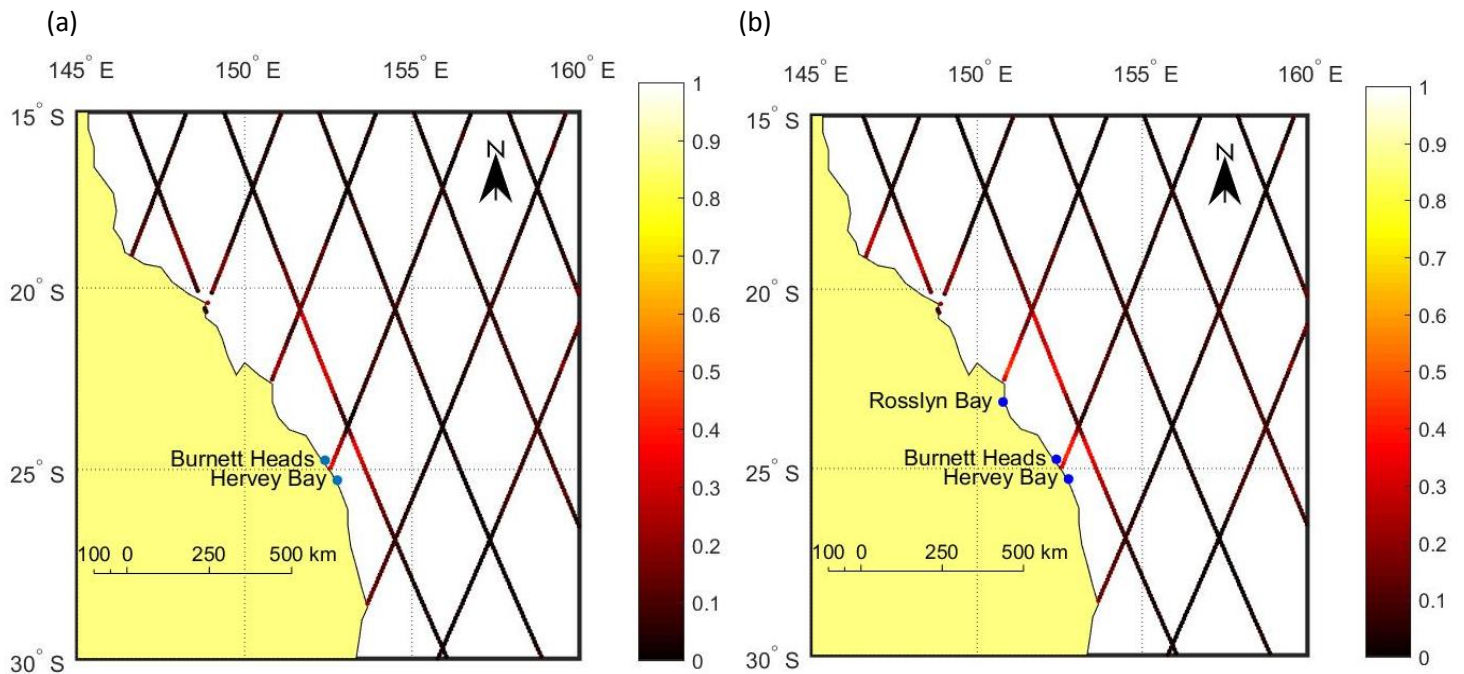


Figure 4.7 – Hindcast skill – (a) Burnett Heads only and (b) Burnett Heads and Roslyn Bay

When the hindcast skill was applied to the model run using only Burnett Heads SLA data, the best results occurred around the location of the tide gauge. These values were around 0.4 to 0.5. This was also the case for all other values predicted close to the coast, with values around the 0.4 mark. The rest of the values further away from the coastline were all close to zero.

The application of the hindcast skill to the predictions involving two sets of tide gauge SLA data showed a slight improvement in the results. Values around the two tide gauges was sitting closer to 0.5, while the rest of the coastline was then covered by a larger area of approximately 0.4. Across the rest of the area, the values stayed close to zero, with an improvement of a much smaller margin.

As the best scenario for the hindcast skill is values close to one, both versions of the model did not perform particularly well. The best performance occurred around the tide gauges,

although this was still not a good performance. The slight improvement of the second run means that the use of two sets of SSH data gives a better performance of the model, although only around the tide gauges.

4.2.3 Validation

Finally, a comparison of measured and predicted data was graphed to validate the model (Figure 4.8). The measured values at the Urangan tide gauge were plotted against the predicted values at the closest point on the satellite tracks (24.9°S, 152.6°E), between the 10th of January 2013 and the 5th of February 2013. This covers the duration of tropical Cyclone Oswald, as well one week either side.

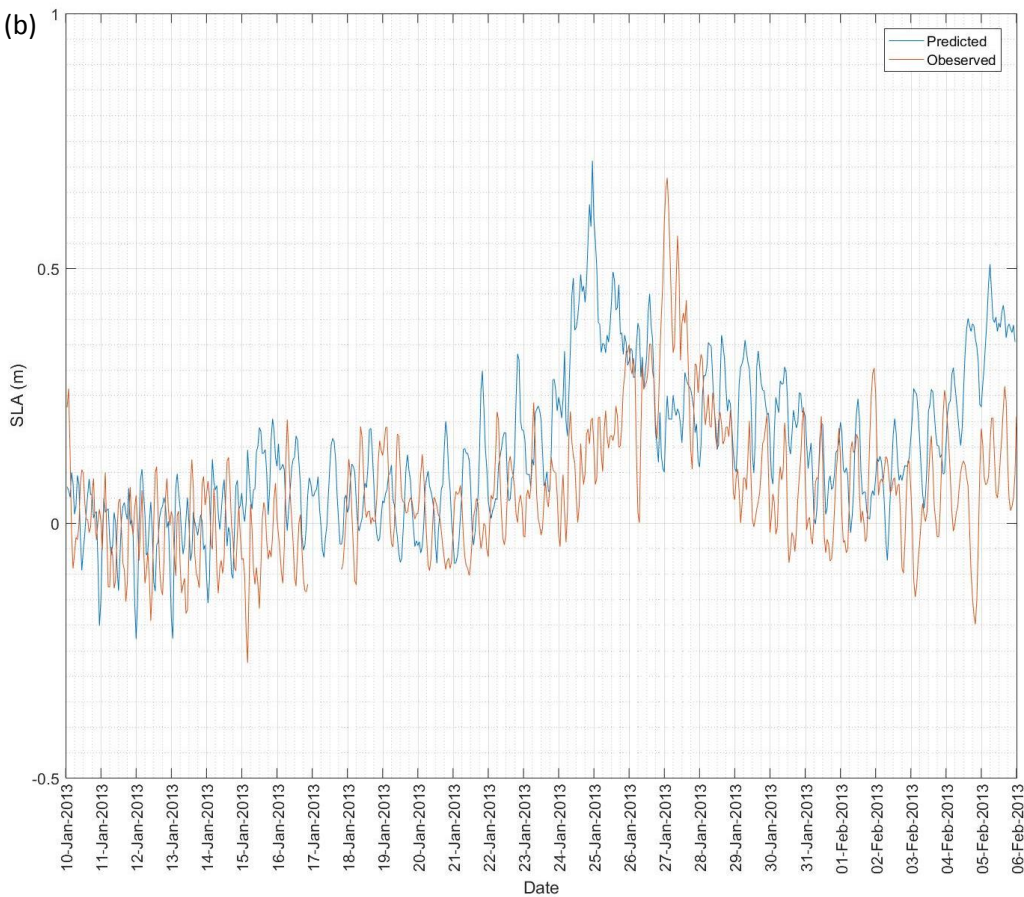
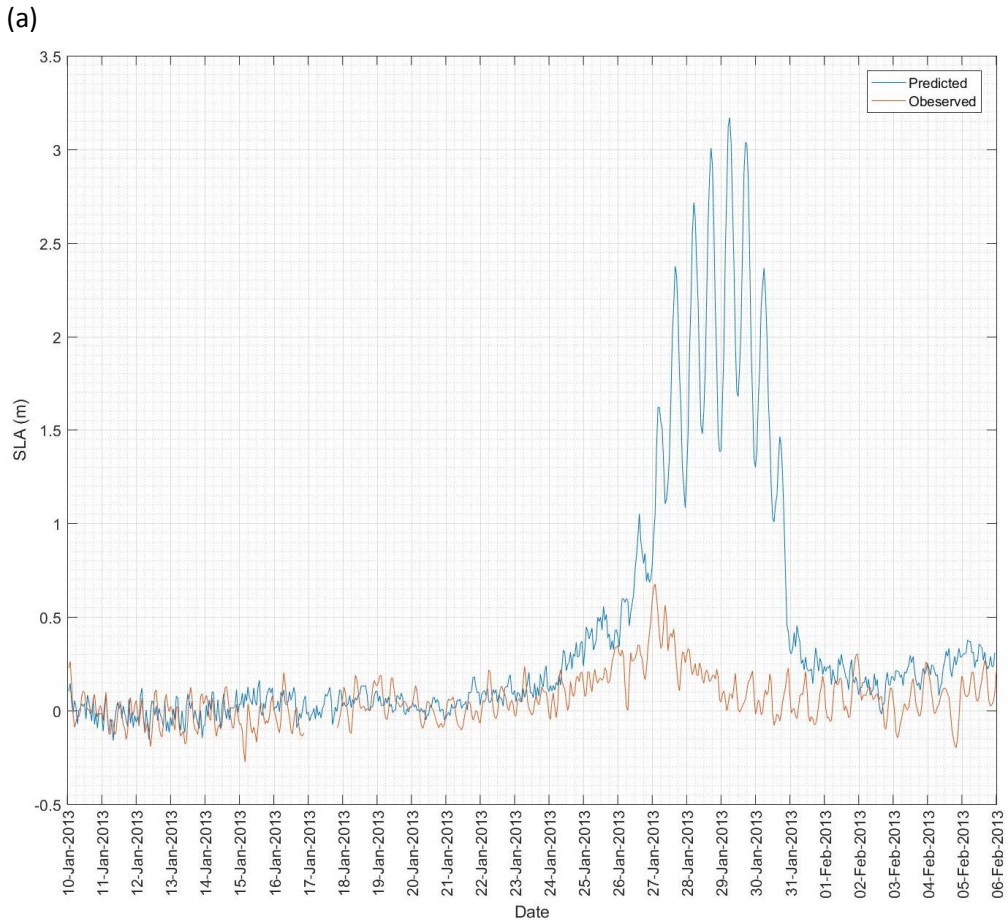


Figure 4.8 – Comparison of measured SLAs at Urangan and predicted SLAs using (a) Burnett Heads only and (b) Burnett Heads and Rosslyn Bay

For both runs of the model, the validation showed a delay between the predicted and the measured SLA data. For the first run (using Burnett Heads only), the peak of the predicted SLAs occurred two days after the measured data. This was due to the delay between the data measured at Burnett Heads and Urangan, with the peak at Burnett Heads occurring two days later. The delay between Rosslyn Bay and Urangan was then seen in the second run (using Burnett Heads and Rosslyn Bay), with the predicted data peaking approximately two days before the measured data. This delay follows the delay between Rosslyn Bay and Urangan.

Both the Burnett Heads and the Burnett Heads/Rosslyn Bay SLA predictions were also able to predict SLAs for the period of missing data from the Urangan tide gauge. The SSH data was not recorded by the Urangan tide gauge for twenty-two hours, from 9:00 pm on the 16th of January to 7:00 pm on the 17th of January. This shows that the model can be used to predict SLA data which was not captured by the tide gauge, as well as help predict changes in SSH during future tropical cyclones.

When taking the time delay into account, both validations showed that the predicted SLAs matched well to the measured SLAs. The only instance where this did not occur was during the SLA peak predicted only using Burnett Heads SLA data. This peak, which occurred between the 25th and the 30th of January, predicted a SLA six times larger than what was measured (approximately 0.5 m measured, 3 m predicted). As Burnett Heads and Urangan did not record the same variation in SSH during this period, the predicted SLAs were therefore not able to fully represent what occurred around the Urangan tide gauge.

Rosslyn Bay, on the other hand, recorded variations in SSH which were much closer to what occurred around Urangan. Using both Burnett Heads and Rosslyn Bay SLA data was

therefore able to predict the changes in SLA more accurately. This shows that using two sets of SLA data gives a better result than only using one.

5 Discussion

The following sections discuss the results presented in the last section. This includes the overall performance of the model, as well as how these results compare to previous research. The limitations of the model are then outlined. Finally, the improvements which could be made to the data used by the model and any future research which stems from this is discussed.

5.1 Multivariate Regression Model

Overall, both runs of the model were able to predict changes in SSH across the selected area. In particular, the use of two sets of tide gauge data gave a more accurate result than the use of one. Both the predictions and the performance of the model showed the best results around the locations of the tide gauges compared to the results achieved further away from the coastline.

The results and the performance, however, were not as good as they could have been. One of the main reasons for this was the number of tide gauges used, as the use of one, then two tide gauges is representative of a small area. The use of more tide gauges in the model giving better results has been shown here, and can also be seen when comparing these results to the research completed by Deng et al. (2015). In this research, 7 tide gauges across the northern side of Australia were used in the model. The correlation which was achieved around the tide gauges was greater than 0.9, with an overall correlation greater than 0.6.

5.2 Limitations

There are a number of limitations which the model has when it comes to predicting results.

One such limitation is the distance between the tide gauge where the predictions are

occurring and the data points measured by the satellite altimeters. As the closest point on the satellite altimeter's track can be hundreds of kilometres away from the tide gauge, it can result in the predictions not occurring at the same time, or under the same conditions, as the data measured at the tide gauge. This would be particularly relevant when using a smaller number of tide gauges, as these conditions would have a higher chance of not being captured by a tide gauge.

Another limitation when using a smaller number of tide gauges is that the model does not take into account the time differences between tide gauges. This means that the time delay would have to be incorporated after the model has been run. There could also be a time delay in the situation mentioned in the last paragraph, depending on how large the distance is, which would also need to be considered.

5.3 Improvements/Future Directions

In order for better results to be achieved by the model when using a smaller number of tide gauges, there are some improvements which may need to be made. The main issue is the relatively low correlation between the measured SSH from the tide gauges and the satellite altimeters, which lead to the model not performing well. This correlation would increase as the technology involved with measuring the SSHs increases in accuracy. Ways to deal with shallow-water gravity anomalies is being researched (e.g. Hwang & Hsu 2008; Khaki et al. 2015), which would help improve the results along the coastline. Improvements are being continuously made to tide gauges, as well as the addition of new tide gauges along the coastline.

The correlation between predicted and measured SLAs may also increase depending on the tide gauge data used, as well as the number of tide gauges used. As demonstrated above,

Rosslyn Bay recorded changes in SSH which were similar to Urangan. When combined with Burnett Heads SLA data, the model results improved slightly, and the model performed better. It could therefore be predicted that using a tide gauge with similar SSH variation to the selected area could improve the model's performance.

6 Conclusion

Tropical cyclones are one of many climatic phenomena that are present around Australia, and can also be seen around other countries which are located near the tropical waters around the equator. Tropical cyclones can have a large impact on the areas they pass over, resulting in excessive rainfall, flooding and storm surges. This was seen during and after tropical cyclone Oswald, through the changes in SSH, the amount of rainfall and the volume of stream discharge which occurred around Queensland.

Through the application of the multivariate regression model, the hourly SLAs from satellite altimetry data was predicted. This meant that hourly SLAs could be given further away from the coastline, and capture changes in SLAs during a tropical cyclone. The model was run using SLA data from one, then two, tide gauges, with the correlation between predicted and measured data giving a better result close to the coast (approximately 0.6, compared to 0.2 away from the shore).

This meant that a better prediction from the model occurred along the coastline. This was proven by the tests of the performance of the model. The comparison of measured SLAs at Urangan to the results of model then showed that the model was capable of predicting missing data, although the run of the model using both Burnett Heads and Rosslyn Bay SLA data was the only one which accurately captured the SSH changes during tropical cyclone Oswald. Due to this, this model would be beneficial for predicting changes in SSHs during a tropical cyclone and, as a result, help in forecasting tropical cyclone impacts along the coastline. More research would need to be completed into improving the performance of the model, in order to ascertain the best results when using a small number of tide gauges.

7 Bibliography

- Arblaster, JM, Jubb, I, Braganza, K, Alexander, LV, Karoly, D & Colman, R 2015, *Weather extremes and climate change - The science behind the attribution of climatic events*, Commonwealth Scientific and Industrial Research Organisation (CSIRO) and Bureau of Meteorology (BOM), Australia, viewed 17/10/2016 <http://www.cawcr.gov.au/projects/climatechange/docs/Weather_Extremes_Report-FINAL.pdf>.
- BOM 2003, *Paths of Tropical Cyclones*, Bureau of Meteorology (BOM), Melbourne, <<http://www.bom.gov.au/cyclone/climatology/wa.shtml>>.
- BOM 2013a, *Ex-TC Oswald Floods - January and February 2013*, Bureau of Meteorology (BOM), Melbourne, viewed 15/03/2016 <http://www.bom.gov.au/qld/flood/fld_reports/EXTC_Oswald.pdf>.
- BOM 2013b, *Monthly Weather Review - Queensland - January 2013*, Bureau Of Meteorology (BOM), Brisbane, viewed 28/03/16 <<http://www.bom.gov.au/climate/mwr/qld/mwr-qld-201301.pdf>>.
- BOM 2013c, *Monthly Weather Review - New South Wales - January 2013*, Bureau Of Meteorology (BOM), Darlinghurst, viewed 28/03/16 <<http://www.bom.gov.au/climate/mwr/nsw/mwr-nsw-201301.pdf>>.
- BOM 2014, *Annual Climate Report 2013*, Bureau of Meteorology (BOM), Melbourne, viewed 28/03/16 <http://www.bom.gov.au/climate/annual_sum/2013/AnClimSum2013_LR1.0.pdf>.
- Chan, JCL 2005, 'THE PHYSICS OF TROPICAL CYCLONE MOTION', *Annual Review of Fluid Mechanics*, vol. 37, no. 1, pp. 99-128.
- Chiew, FHS, Piechota, TC, Dracup, JA & McMahon, TA 1998, 'El Nino/Southern Oscillation and Australian rainfall, streamflow and drought: Links and potential for forecasting', *Journal of Hydrology*, vol. 204, no. 1, pp. 138-49.
- Collilieux, X & Wöppelmann, G 2010, 'Global sea-level rise and its relation to the terrestrial reference frame', *Journal of Geodesy*, vol. 85, no. 1, pp. 9-22.
- CSIRO & BOM 2015, *Climate Change in Australia - Technical Report*, Commonwealth Scientific and Industrial Research Organisation (CSIRO) and Bureau of Meteorology (BOM), Australia, viewed 28/03/2016 <http://www.climatechangeinaustralia.gov.au/media/ccia/2.1.5/cms_page_media/168/CCIA_2015_NRM_TechnicalReport_WEB.pdf>.
- Dare, RA 2013, 'Seasonal Tropical Cyclone Rain Volumes over Australia', *Journal of Climate*, vol. 26, no. 16, pp. 5958-64.
- Dare, RA & McBride, JL 2011, 'The Threshold Sea Surface Temperature Condition for Tropical Cyclogenesis', *Journal of Climate*, vol. 24, no. 17, pp. 4570-6.
- Deng, X, Gharineiat, Z, Andersen, OB & Stewart, MG 2015, 'Observing and Modelling the High Water Level from Satellite Radar Altimetry During Tropical Cyclones', in Springer Berlin Heidelberg, Berlin, Heidelberg, pp. 1-9.
- Emanuel, K 2003, 'TROPICAL CYCLONES', *Annual Review of Earth & Planetary Sciences*, vol. 31, no. 1, p. 75.
- Emery, WJ & Thomson, RE 2001, *Data analysis methods in physical oceanography*, 2nd and rev. ed. edn, Elsevier, Amsterdam.
- Engel, CB, Lane, TP, Reeder, MJ & Reznay, M 2013, 'The meteorology of Black Saturday', *Quarterly Journal of the Royal Meteorological Society*, vol. 139, no. 672, pp. 585-99.
- Gharineiat, Z & Deng, X 2015, 'Application of the Multi-Adaptive Regression Splines to Integrate Sea Level Data from Altimetry and Tide Gauges for Monitoring Extreme Sea Level Events', *Marine Geodesy*, vol. 38, no. 3, pp. 261-76.
- Granger, K, Hayne, M, Jones, T, Middlemann, MH, Leiba, M & Scott, G 2001, *Natural Hazards & the risks they pose to Southeast Queensland*, Geoscience Australia, Canberra, viewed 01/04/16 <https://d28rz98at9flks.cloudfront.net/37282/Rec_2001_29.pdf>.

Haigh, ID, MacPherson, LR, Mason, MS, Wijeratne, EMS, Pattiaratchi, CB, Crompton, RP & George, S 2013, 'Estimating present day extreme water level exceedance probabilities around the coastline of Australia: tropical cyclone-induced storm surges', *Climate Dynamics*, vol. 42, no. 1, pp. 139-57.

Haynes, K, Handmer, J, McAneney, J, Tibbits, A & Coates, L 2010, 'Australian bushfire fatalities 1900–2008: exploring trends in relation to the 'Prepare, stay and defend or leave early' policy', *Environmental Science & Policy*, vol. 13, no. 3, pp. 185-94.

Hicks, SD 2006, *UNDERSTANDING TIDES*, National Oceanic and Atmospheric Administration, Center for Operational Oceanographic Products and Services (CO-OPS). viewed 16/09/2016
<https://tidesandcurrents.noaa.gov/publications/Understanding_Tides_by_Steacy_finalFINAL11_30.pdf>.

Høyer, JL & Andersen, OB 2003, 'Improved description of sea level in the North Sea', *Journal of Geophysical Research: Oceans*, vol. 108, no. C5, pp. n/a-n/a.

Hwang, C & Hsu, HY 2008, 'Shallow-water gravity anomalies from satellite altimetry: Case studies in the east china sea and Taiwan strait', *Journal of the Chinese Institute of Engineers*, vol. 31, no. 5, pp. 841-51.

Ji, F, Evans, JP, Argueso, D, Fita, L & Di Luca, A 2015, 'Using large-scale diagnostic quantities to investigate change in East Coast Lows', *Climate Dynamics*, vol. 45, no. 9, pp. 2443-53.

Jones, SC, Harr, PA, Abraham, J, Bosart, LF, Bowyer, PJ, Evans, JL, Hanley, DE, Hanstrum, BN, Hart, RE, Lalaurette, F, Sinclair, MR, Smith, RK & Thorncroft, C 2003, 'The Extratropical Transition of Tropical Cyclones: Forecast Challenges, Current Understanding, and Future Directions', *Weather & Forecasting*, vol. 18, no. 6, pp. 1052-92.

Khaki, M, Forootan, E, Sharifi, MA, Awange, J & Kuhn, M 2015, 'Improved gravity anomaly fields from retracked multimission satellite radar altimetry observations over the Persian Gulf and the Caspian Sea', *Geophysical Journal International*, vol. 202, no. 3, pp. 1522-34.

Knaff, JA, Brown, DP, Courtney, J, Gallina, GM & Beven, JL 2010, 'An Evaluation of Dvorak Technique-Based Tropical Cyclone Intensity Estimates', *Weather & Forecasting*, vol. 25, no. 5, pp. 1362-79.

Lambin, J, Morrow, R, Fu, L-L, Willis, JK, Bonekamp, H, Lillibridge, J, Perbos, J, Zaouche, G, Vaze, P, Bannoura, W, Parisot, F, Thouvenot, E, Coutin-Faye, S, Lindstrom, E & Mignogno, M 2010, 'The OSTM/Jason-2 Mission', *Marine Geodesy*, vol. 33, no. sup1, pp. 4-25.

Leigh, C, Bush, A, Harrison, ET, Ho, SS, Luke, L, Rolls, RJ & Ledger, ME 2015, 'Ecological effects of extreme climatic events on riverine ecosystems: insights from Australia', *Freshwater Biology*, vol. 60, no. 12, pp. 2620-38.

Madsen, KS, Høyer, JL, Fu, W & Donlon, C 2015, 'Blending of satellite and tide gauge sea level observations and its assimilation in a storm surge model of the North Sea and Baltic Sea', *Journal of Geophysical Research: Oceans*, vol. 120, no. 9, pp. 6405-18.

McAneney, J, Chen, K & Pitman, A 2009, '100-years of Australian bushfire property losses: Is the risk significant and is it increasing?', *Journal of Environmental Management*, vol. 90, no. 8, pp. 2819-22.

Meyers, G, McIntosh, P, Pigot, L & Pook, M 2007, 'The Years of El Niño, La Niña, and Interactions with the Tropical Indian Ocean', *Journal of Climate*, vol. 20, no. 13, pp. 2872-80.

Middelmann, MH 2007, *Natural Hazards in Australia - Identifying Risk Analysis Requirements*, Geoscience Australia, Canberra, viewed 10/10/2016,
<<https://d28rz98at9flks.cloudfront.net/65444/65444.pdf>>.

Munk, WH & Cartwright, DE 1966, 'Tidal Spectroscopy and Prediction', *Philosophical Transactions of the Royal Society of London. Series A, Mathematical and Physical Sciences*, vol. 259, no. 1105, pp. 533-81.

PCTMSL 2011, *Australian Tides Manual - Special Publication No. 9*, Permanent Committee on Tides and Mean Sea Level (PCTMSL), Wollongong, Australia, viewed 29/09/2016
<http://www.icsm.gov.au/tides/SP9_Australian_Tides_Manual_V4.1.pdf>.

Pepler, A, Coutts-Smith, A & Timbal, B 2014, 'The role of East Coast Lows on rainfall patterns and inter-annual variability across the East Coast of Australia', *International Journal of Climatology*, vol. 34, no. 4, pp. 1011-21.

- Perkins-Kirkpatrick, SE, White, CJ, Alexander, LV, Argüeso, D, Boschat, G, Cowan, T, Evans, JP, Ekström, M, Oliver, ECJ, Phatak, A & Purich, A 2016, 'Natural hazards in Australia: heatwaves', *Climatic Change*, pp. 1-14.
- Preen, A & Marsh, H 1995, 'Response of dugongs to large-scale loss of seagrass from Hervey Bay, Queensland Australia', *Wildlife Research*, vol. 22, no. 4, pp. 507-19.
- Preen, AR, Lee Long, WJ & Coles, RG 1995, 'Flood and cyclone related loss, and partial recovery, of more than 1000 km² of seagrass in Hervey Bay, Queensland, Australia', *Aquatic Botany*, vol. 52, no. 1-2, pp. 3-17.
- Purich, A, Cowan, T, Cai, W, van Rensch, P, Uotila, P, Pezza, A, Boschat, G & Perkins, S 2014, 'Atmospheric and Oceanic Conditions Associated with Southern Australian Heat Waves: A CMIP5 Analysis', *Journal of Climate*, vol. 27, no. 20, pp. 7807-29.
- Risbey, JS, Pook, MJ, McIntosh, PC, Wheeler, MC & Hendon, HH 2009, 'On the Remote Drivers of Rainfall Variability in Australia', *Monthly Weather Review*, vol. 137, no. 10, pp. 3233-53.
- Roy, C & Kovordányi, R 2012, 'Tropical cyclone track forecasting techniques — A review', *Atmospheric Research*, vol. 104-105, pp. 40-69.
- Saha, K 2010, *Tropical Circulation Systems and Monsoons*, Springer Berlin Heidelberg, Berlin, Heidelberg.
- SDMG 2013, *Tropical Cyclone Storm Tide Warning – Response System Handbook 11th Edition* State Disaster Management Group (SDMG) & The Bureau of Meteorology, Brisbane, viewed 02/04/2016 <<http://www.disaster.qld.gov.au/disaster-resources/documents/storm-tide-handbook.pdf>>.
- Shum, CK, Ries, JC & Tapley, BD 1995, 'The accuracy and applications of satellite altimetry', *Geophysical Journal International*, vol. 121, no. 2, pp. 321-36.
- Steffen, W, Hughes, L & Karoly, D 2013, *The Critical Decade: Extreme Weather*, Climate Council, viewed 28/03/2016 <<http://www.climatecouncil.org.au/uploads/94e1a6db30ac7520d3bbb421322b4dfb.pdf>>.
- Ummenhofer, CC, Sen Gupta, A, Briggs, PR, England, MH, McIntosh, PC, Meyers, GA, Pook, MJ, Raupach, MR & Risbey, JS 2011, 'Indian and Pacific Ocean Influences on Southeast Australian Drought and Soil Moisture', *Journal of Climate*, vol. 24, no. 5, pp. 1313-36.
- van Dijk, AIJM, Beck, HE, Crosbie, RS, de Jeu, RAM, Liu, YY, Podger, GM, Timbal, B & Viney, NR 2013, 'The Millennium Drought in southeast Australia (2001–2009): Natural and human causes and implications for water resources, ecosystems, economy, and society', *Water Resources Research*, vol. 49, no. 2, pp. 1040-57.
- Villarini, G & Denniston, RF 2016, 'Contribution of tropical cyclones to extreme rainfall in Australia', *International Journal of Climatology*, vol. 36, no. 2, pp. 1019-25.
- Zhao, D & Toba, Y 2002, 'A Spectral Approach for Determining Altimeter Wind Speed Model Functions', *Journal of Oceanography*, vol. 59, no. 2, pp. 235-44.